

WL-TR-97-3045



BUCKDEL v 0.9 USERS AND THEORY MANUALS

Buckling and Delamination Analysis of Stiffened Laminated Plates

D.S. PIPKINS
S.N. ATLURI

Knowledge Systems, Inc.,
81 E. Main St.
Forsyth, GA 31029

APRIL 1996

FINAL REPORT FOR THE PERIOD SEPTEMBER 1995 - MARCH 1996

APPROVED FOR PUBLIC RELEASE; DISTRIBUTION IS UNLIMITED

FLIGHT DYNAMICS DIRECTORATE
WRIGHT LABORATORY
AIR FORCE MATERIEL COMMAND
WRIGHT-PATTERSON AIR FORCE BASE, OHIO 45433-7552

19970801 047


THIS DOCUMENT CONTAINS UNCLASSIFIED INFORMATION

NOTICE

WHEN GOVERNMENT DRAWINGS, SPECIFICATIONS, OR OTHER DATA ARE USED FOR ANY PURPOSE OTHER THAN IN CONNECTION WITH A DEFINITE GOVERNMENT-RELATED PROCUREMENT, THE UNITED STATES GOVERNMENT INCURS NO RESPONSIBILITY OR ANY OBLIGATION WHATSOEVER. THE FACT THAT THE GOVERNMENT MAY HAVE FORMULATED OR IN ANY WAY SUPPLIED THE SAID DRAWING, SPECIFICATIONS OR OTHER DATA, IS NOT TO BE REGARDED BY IMPLICATION, OR OTHERWISE IN ANY MANNER CONSTRUED, AS LICENSING THE HOLDER, OR ANY OTHER PERSON OR CORPORATION; OR AS CONVEYING ANY RIGHTS OR PERMISSION TO MANUFACTURE, USE, OR SELL ANY PATENTED INVENTION THAT MAY IN ANY WAY BE RELATED THERETO.

THIS REPORT IS RELEASABLE TO THE NATIONAL TECHNICAL INFORMATION SERVICE (NTIS). AT NTIS, IT WILL BE AVAILABLE TO THE GENERAL PUBLIC, INCLUDING FOREIGN NATIONS.

THIS TECHNICAL REPORT HAS BEEN REVIEWED AND IS APPROVED FOR PUBLICATION.



Victoria A. Tischler
Project Engineer
Design and Analysis Branch



Peter M. Flick, Principal Engineer
Design and Analysis Branch



Nelson Wolf, Acting Chief
Design and Analysis Branch
Structures Division

IF YOU ADDRESS HAS CHANGED, IF YOU WISH TO BE REMOVED FROM OUR MAILING LIST, OR IF THE ADDRESSEE IS NO LONGER EMPLOYED BY YOUR ORGANIZATION, PLEASE NOTIFY WL/FIBD BLDG 45, 2130 EIGHTH STREET, SUITE 1, WRIGHT-PATTERSON AFB OH 45433-7552 TO HELP MAINTAIN A CURRENT MAILING LIST.

Copies of this report should not be returned unless return is required by security considerations, contractual obligations, or notice on a specified document.

REPORT DOCUMENTATION PAGE			Form Approved OMB No. 0704-0188	
Public reporting burden for this collection of information is estimated to average 1 hour per response, including the time for reviewing instructions, searching existing data sources, gathering and maintaining the data needed, and completing and reviewing the collection of information. Send comments regarding this burden estimate or any other aspect of this collection of information, including suggestions for reducing this burden, to Washington Headquarters Services, Directorate for Information Operations and Reports, 1215 Jefferson Davis Highway, Suite 1204, Arlington, VA 22202-4302, and to the Office of Management and Budget, Paperwork Reduction Project (0704-0188), Washington, DC 20503.				
1. AGENCY USE ONLY (Leave blank)		2. REPORT DATE APR 1996		3. REPORT TYPE AND DATES COVERED FINAL 09/29/95 - 04/29/96
4. TITLE AND SUBTITLE BUCKDEL v. 0.9 USERS AND THEORY MANUALS BUCKLING AND DELAMINATION ANALYSIS OF STIFFENED LAMINATED PLATES			5. FUNDING NUMBERS CONTR: F33615-95-C-3226 PE 65502 PR 3005 TA 41 WU 38	
6. AUTHOR(S) D.S. Pipkins and S.N. Atluri				
7. PERFORMING ORGANIZATION NAME(S) AND ADDRESS(ES) Knowledge Systems, Inc. 81 East Main Street Forsyth, GA 31029-1828			8. PERFORMING ORGANIZATION REPORT NUMBER	
9. SPONSORING/MONITORING AGENCY NAME(S) AND ADDRESS(ES) FLIGHT DYNAMICS DIRECTORATE WRIGHT LABORATORY QIR FORCE MATERIEL COMMAND WRIGHT PATTERSON AFB, OH 45433-7562 POC: VICTORIA A. TISCHLER WL/FIBD (937) 255-6992			10. SPONSORING/MONITORING AGENCY REPORT NUMBER WL-TR-97-3045	
11. SUPPLEMENTARY NOTES				
12a. DISTRIBUTION / AVAILABILITY STATEMENT Approved for public release; distribution unlimited.			12b. DISTRIBUTION CODE	
13. ABSTRACT (Maximum 200 words) BUCKDEL, performs geometrically nonlinear analysis of stiffened laminated composite plates with and without delaminations. BUCKDEL allows the user to perform: a linear static solution; a linear buckling (eigenvalue) analysis; and a nonlinear post-buckling analysis through both limit and bifurcation points. There are two finite elements in BUCKDEL; a quasi-conforming triangular laminated plate element based on a refined first order shear theory with seven degrees of freedom per node and a fiber-reinforced beam element with seven degrees of freedom per node. The behavior of all materials is assumed to be linearly elastic. The multi-domain modeling method is used for the analysis of laminated plates containing delaminations. In this model, the delaminate, base and the undelaminate are modeled as 3 distinct. On the delamination front, Mindlin's deformation assumption is applied to obtain the relationship between the displacements in the delaminate, base and undelaminate.				
14. SUBJECT TERMS BUCKDEL, LAMINATED COMPOSITE, DELAMINATIONS, BUCKLING, POST-BUCKLING, LIMIT AND BIFURCATION POINTS, MULTI-DOMAIN MODELING METHOD, FINITE ELEMENT METHOD			15. NUMBER OF PAGES 50	
			16. PRICE CODE	
17. SECURITY CLASSIFICATION OF REPORT UNCLASSIFIED	18. SECURITY CLASSIFICATION OF THIS PAGE UNCLASSIFIED	19. SECURITY CLASSIFICATION OF ABSTRACT UNCLASSIFIED	20. LIMITATION OF ABSTRACT	

BUCKDEL v0.9 Users Manual

Buckling and Delamination Analysis of Stiffened Laminated Plates

Knowledge Systems, Inc.
81 East Main St.
Forsyth, GA 31029
April 1996

Contents

1 INTRODUCTION	1
2 DISK CONTENTS AND INSTALLATION PROCEDURE	1
3 RUNNING BUCKDEL	2
4 RUNNING BUCKGEN	2
4.1 Introduction	2
4.2 BUCKGEN Main Menu	3
4.3 Problem "Dependent" Control Parameters Not Set by BUCKGEN	6
5 BUCKDEL INPUT FILE FORMAT	7
6 OUTPUT FILES	21
7 EXAMPLE PROBLEMS	22
7.1 Simply Supported Laminated Plate Under Biaxial Compression	22
7.2 Simply Supported Laminated Plate with Delamination	24

BUCKDEL v0.9 Theory Manual

Buckling and Delamination Analysis of Stiffened Laminated Plates

Knowledge Systems, Inc.
81 East Main St.
Forsyth, GA 31029
April 1996

Contents

1	INTRODUCTION	27
2	DELAMINATIONS IN LAMINATED COMPOSITE MATERIALS	28
3	MULTI-DOMAIN MODELING OF DELAMINATIONS	30
4	FINITE ELEMENT FORMULATIONS	35
4.1	BEAM2: 2-noded curved beam element	35
4.2	SHELL3: 3-noded triangular curved shell element	35
5	NONLINEAR SOLUTION SCHEMES	40
6	POINTWISE ENERGY RELEASE RATE CALCULATION	41

1 Introduction

The BUCKDEL software package consists of two programs. The first program is called BUCKGEN and it is used to generate the input data file for the main program. The main program, called BUCKDEL, performs geometrically nonlinear analysis of stiffened laminated composite plates with and without delaminations. BUCKDEL allows the user to perform:

- a linear static solution;
- a linear buckling (eigenvalue) analysis; and
- a nonlinear post-buckling analysis through both limit and bifurcation points.

There are two finite elements in BUCKDEL; a quasi-conforming triangular laminated plate element based on a refined first order shear theory with seven degrees of freedom per node and a fiber-reinforced beam element with seven degrees of freedom per node. The behavior of all materials is assumed to be linearly elastic.

The multi-domain modeling method is used for the analysis of laminated plates containing delaminations. In this model, the delaminate, base and the undelaminate are modeled as 3 distinct plates (see Figure 1-1). On the delamination front, Mindlin's deformation assumption is applied to obtain the relationship between the displacements in the delaminate, base and undelaminate.

V1
L1
C1

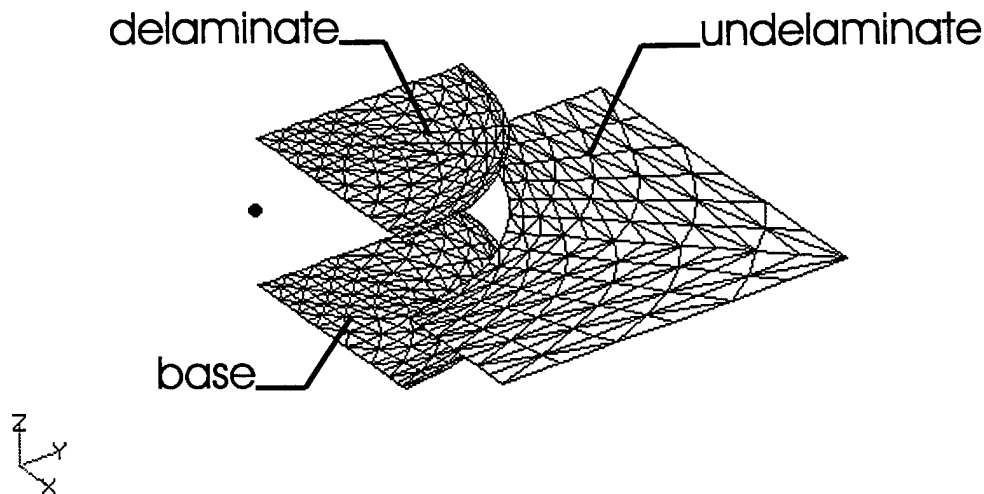


Figure 1-1: Multi-domain model of a laminated plate containing a delamination

2 Disk Contents and Installation Procedure

This section describes the steps that must be followed to use the BUCKDEL software package. The disk accompanying this manual contains:

1. executable versions of BUCKGEN (**buckgen.exe**) and BUCKDEL (**buckdel.exe**);

2. sample input files; and
3. the file **readme.txt**.

The sample input files are described in Section 7 of this manual. They can be used to verify that BUCKDEL is functioning correctly on your system once it is installed. The file **readme.txt** contains installation and program execution instructions specific to your machine. All the files on the disk should be loaded onto your computer. It will be convenient to create a separate directory for these files. The procedure required to load these files onto your computer will be system dependent.

3 Running BUCKDEL

To execute BUCKDEL, the user must first create an input data file. Therefore, the interactive input file generator, BUCKGEN, must be run prior to executing BUCKDEL. The procedures for running BUCKGEN are described in detail in Section 4. While BUCKGEN automates the creation of the BUCKDEL input file, **there are several input file parameters which must be manually added by the user**. These are discussed in Section 4.3. The structure of the BUCKDEL input file created by BUCKGEN is described in detail in Section 5. Once an input data file has been prepared, BUCKDEL is easy to run. When BUCKDEL is executed, the user is prompted for the name of the input file. BUCKDEL reads the specified input file and execution proceeds. During execution, various output files are created by BUCKDEL. These depend to some extent on the analysis option chosen and are described in Section 6.

4 Running BUCKGEN

4.1 Introduction

BUCKGEN is an interactive pre-processor that creates data files that are used as input to BUCKDEL. The following are several general comments on the operation of BUCKGEN. It is important that the user be familiar with these prior to running BUCKGEN.

- To initiate BUCKGEN, the user simply types **buckgen.exe**.
- The input for BUCKGEN is primarily carried out by stepping through a series of input menus, each containing several options. Once a particular option is selected, the program will issue a number of prompts to the user requesting that data be entered or that additional options be selected. Data can be easily modified or changed by re-selecting a particular option at a later stage.
- Items from a menu are selected by entering the number corresponding to a particular item.
- BUCKGEN contains many features that will assist the user in generating an input file for BUCKDEL. For example, there are a number of warning messages advising the user when the input data is inconsistent with that

expected. Because of its interactive nature, the program allows the user to re-enter the data when such a warning message is received.

4.2 BUCKGEN Main Menu

The main menu, which appears when BUCKGEN is initiated, contains three options. The user selects the desired option by entering the appropriate number. These options are as follows.

- 1 :Control Data
- 2 :Mesh Generation Data
- 3 :Exit BUCKGEN

When creating a data file, the user must select some or all of these options. **Option 1 must always be selected prior to all other options** and this option must be completed before proceeding to the other options. The remaining options can be carried out in a random order.

4.2.1 BUCKGEN Input Menu 1: Control Data

Various control parameters required by BUCKGEN and BUCKDEL are entered from Input Menu 1, which appears when item 1 is selected from the Main Menu. Input Menu 1 contains four options. These options are as follows.

- 1 :Enter Problem Title
- 2 :Enter Output File Name (REQUIRED)
- 3 :Enter Analysis Option
- 4 :Return to Main Menu

The user must complete this menu before proceeding with any other portions of the data file generation. Note that Option 2 must be completed.

4.2.1.1 Option 1: Enter Problem Title

When this option is selected, the user is prompted for a problem title. This option is for the benefit of the user and may be skipped. The title must be less than sixty characters.

4.2.1.2 Option 2: Enter Output File Name

The user must always select a name for the output file. This can have the same name as an existing file or it can be a new file. It must be less than twenty characters in length.

4.2.1.3 Option 3: Enter Analysis Option

When this option is selected, a new menu appears containing the analysis choices. The analysis choices are as follows.

- 1 :Linear analysis
- 2 :Linear and buckling analysis
- 3 :Buckling and post-buckling analysis
- 4 :Nonlinear analysis through both limit and bifurcation points
- 5 :Nonlinear analysis through limit points only

When a selection is made, control automatically reverts back to Input Menu 1.

4.2.1.4 Option 4: Return to Main Menu

Select this option in order to return to the Main Menu.

4.2.2 BUCKGEN Input Menu 2: Mesh Generation Data

The data defining the finite element model is entered through Input Menu 2. The data (i.e. nodes, element connectivities, material and geometric properties and boundary conditions) is imported from a file which is in a NASTRAN bulk data file format. The options in Input Menu 2 are as follows.

- 1 :Translate Finite Element Model Data File
- 2 :View Nodal Coordinates
- 3 :View Element Connectivities
- 4 :Optimize Node Numbering
- 5 :Return to Main Menu

4.2.2.1 Option 1: Translate Finite Element Model Data File

BUCKGEN has been set up to read finite element model data from a NASTRAN bulk data file and translate it into a form which BUCKDEL can use. Thus, any finite element pre-processor which can write a file in this format can be used in conjunction with the BUCKDEL package. The bulk data file should contain only information about nodes, element connectivities, material and geometric properties and boundary conditions. The file should begin with "BEGIN BULK" and end with "ENDDATA". The bulk data mnemonics which are supported are: GRID, CTRIA3, CBAR, MAT1, MAT8, PSHELL, PBAR, PCOMP, FORCE,

SPC, and SPC1. In addition, the mnemonics \$, PARAM, and CORD are read by BUCKGEN but data associated with them is not used. For proper translation to take place, the following guidelines should be observed when creating the finite element model.

- The finite element model should be created using a single Cartesian coordinate system.
- The finite element model should be created in the x - y plane.
- The plate should be modeled with 3 noded triangular elements.
- The stiffeners should be modeled with 2 noded beam elements.
- The element connectivities of beam elements should be specified using nodes which are also used to specify the connectivities of triangular elements (i.e. there should not be any nodes which are referenced by beam elements only).
- The finite element model should have consecutively numbered nodes and elements, each beginning with number one.
- Non-zero displacement constraints are not permitted.
- Only nodal loads may be applied to the model.
- An isotropic or orthotropic material may be specified for the plate.
- Ply angles are given with respect to the global x -axis.
- Ply angles and thicknesses are assumed to specified from the “bottom” or “- z ” face of the plate.
- An isotropic material must be used for the stiffeners.
- Delaminations are modeled by three distinct plates (see Figure 1). For the purposes of model creation, it is most convenient to create the undelaminate in the $z=0$ plane, the base in the $z=-a$ plane and the delaminate in the $z=a$ plane (a is an arbitrary number). Upon translation, BUCKGEN will map the three plates to the $z=0$ plane.
- The undelaminate should be assigned property number 1, the base property number 2, and the delaminate property number 3.
- The number of plies in the delaminate and base should equal that of the undelaminate.
- The nodes of the undelaminate, base and delaminate on the delamination front should have the same x and y coordinates. After translation by BUCKGEN and mapping of the three plates to the $z=0$ plane, the nodes of the three plates on the delamination front will be coincident.
- The plate elements should be symmetric across the delamination front if energy release rate calculations are being performed (see Cards for Plate Elements in Section 5).
- Stiffeners can't be modeled on base and delaminate plates. They can only be modeled on the undelaminate plate.

When this option is selected, a menu appears which gives the user one choice (translation from other formats will be added in the future).

1 :Translate From NASTRAN Bulk Data File
--

After making a choice, the user is then prompted for a file name. The file name must be less than twenty characters. BUCKGEN will translate the designated file and return to Input Menu 2. During the translation, if data cards are read which BUCKGEN does not recognize, the user will be warned.

4.2.2.2 Option 2: View Nodal Coordinates

The user can view the nodal coordinates of selected nodes by choosing this option. Since the number of nodes in the system is often relatively large, the user may not wish to look at all the data. Instead the user can view a range of nodes. Thus, when the option is selected the user is prompted for the first and last nodes in the range. The coordinates of these nodes are then written to the screen.

4.2.2.3 Option 3: View Element Connectivities

The user can view the connectivities of selected elements by choosing this option. Since the number of elements in the system is often relatively large, the user may not wish to look at all the data. Instead the user can view a range of elements. Thus, when the option is selected, the user is prompted for the first and last elements in the range. The connectivities of these elements are then written to the screen.

4.2.2.4 Option 4: Optimize Node Numbering

This option renumbers the nodes so as to minimize the bandwidth of the problem. While this option does not affect the BUCKDEL result, it is recommended that it be utilized as the problem will require less memory and execute faster. The user should keep in mind that the node numbering of the model imported via Option 1, will be altered.

4.2.2.5 Option 5: Return to Main Menu

Select this option in order to return to the Main Menu.

4.2.3 *BUCKGEN Input Menu 3: Exit BUCKGEN*

Input Menu 3 allows the user to exit the BUCKGEN program and save the generated data in the file specified by the user in Input Menu 1 (by entering a 1). The user can also use this option to quit the program without saving the data (by entering a -1).

4.3 Problem “Dependent” Control Parameters Not Set by BUCKGEN

BUCKGEN takes care of the majority of BUCKDEL input data file creation for the user, including the specification of problem “independent” control parameters. However, there are several problem “dependent” control parameters which the user must set manually. This section lists these parameters. Reference is made to the input data file cards which are described in Section 5.

1. All parameters on Card 5.
2. The parameter ECCEN on Card 7.
3. The parameters N11 and N22 on Card 8, if the problem contains a delamination.

5 BUCKDEL Input File Format

This section describes the BUCKDEL input file format. The file format is described as a series of cards. In addition to the cards described in this section, the input file may also contain any number of comment cards. These comment cards must begin with '***'. As discussed in the previous section, BUCKGEN creates this file for the user. Only the problem "dependent" control parameters described in Section 4.3 must be manually specified by the user. However, the user may wish to change:

- material properties,
- ply orientations,
- solution control parameters,
- output control parameters, etc.

of a specific problem. To do so the user would need to either create a new NASTRAN bulk data file for translation by BUCKGEN, or edit an existing data file. If the latter method is chosen, the information contained in this section will be useful.

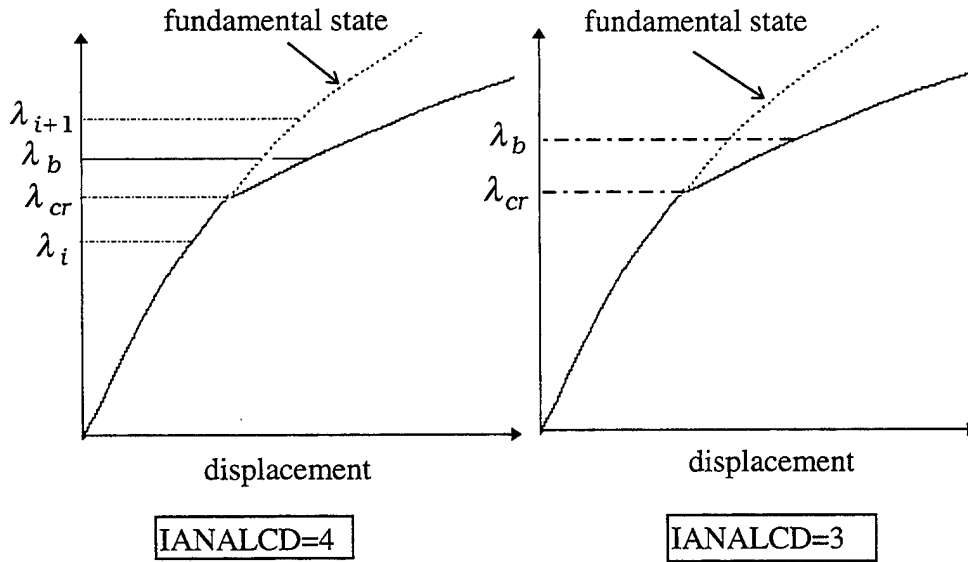
Card 1

Columns	Quantity	Format
1-5	Analysis option (IANALCD) = 1 Linear analysis = 2 Linear and buckling analysis = 3 Buckling and post-buckling analysis = 4 Nonlinear analysis through both limit and bifurcation points = 5 Nonlinear analysis through limit points only	I5
6-10	Number of nodes (NUMNP)	I5
11-15	Number of plate elements (NEQ)	I5
16-20	Number of beam elements (NEL)	I5
21-25	Number of concentrated (nodal) load cards (JS0)	I5

Card 2

Columns	Quantity	Format
1-5	Option between Pure Newton-Raphson and modified Newton-Raphson methods (NEWTON) = 0 All iterations modified Newton-Raphson ≠ 0 first NEWTON iterations with pure Newton-Raphson and after that modified Newton-Raphson iterations	I5
6-10	Maximum number of iterations in each step (MAXR)	I5
11-15	Maximum number of steps before bifurcation (MAXI)	I5
16-20	Maximum number of steps after bifurcation (MAXPB)	I5
21-25	Desired (expected) number of iterations (I0)	I5
26-30	Maximum number of iterations in buckling analysis (ITN)	I5

Columns	Quantity	Format
1-10	Given increment of load factor at bifurcation point (DSMITA) (default = 0.2)	F10.3
11-15	Options for bifurcation path following (KUD) = 1 follow the ascending post-buckling branch = -1 follow the descending post-buckling branch	I5
16-25	Coefficient in the formula for switching post-buckling branches (COEA) (default = 1)	F10.3



The first load point after bifurcation (λ_b) is determined from the user supplied value for DSMITA. When nonlinear analysis through bifurcation points (IANALCD=4) is performed,

$$DSMITA = \frac{\lambda_b - \lambda_{cr}}{\lambda_{cr} - \lambda_i}$$

For buckling and post-buckling analysis (IANALCD=3),

$$DSMITA = \frac{\lambda_b - \lambda_{cr}}{\lambda_{cr}}$$

COEA is used to determine the displacement increment ($\Delta u_b = u_b - u_{cr}$) as given by

$$\Delta u_b = COEA \times A \times u_{buck} \quad \text{for IANALCD=3}$$

$$\Delta u_b = DSMITA \times (u_{i+1} - u_i) + COEA \times A \times u_{buck} \quad \text{for IANALCD=4}$$

u_{buck} is the buckling mode and "A" is determined by the analysis.

Card 4

Columns	Quantity	Format
1-10	Load step factor for the initial step (DDZ1)	F10.3
11-20	Tolerance for the generalized deflection (EE1)	F10.3
21-30	Tolerance for the load factor (EE2)	F10.3
31-40	Maximum allowable increment of the load factor (SKLOAD) load increment \leq SKLOAD \times DDZ1 at any load step	F10.3
41-45	Arc-length method (KARC) = 0 sphere arc-length (Crissfield) = 1 plane arc-length (Riks) = 2 load control method	I5

The convergence conditions in the arc-length are satisfied if

$$\frac{\{F\}^T \{\Delta q_n^i - \Delta q_n^{i-1}\}}{\{F\}^T \{\Delta q_n^i\}} \leq \text{EE1}$$

and

$$\frac{|\Delta \lambda_n^i - \Delta \lambda_n^{i-1}|}{|\Delta \lambda_n^i|} \leq \text{EE2}$$

F , Δq_n^i and $\Delta \lambda_n^i$ are the load vector, displacement vector increment and load vector increment, respectively, at the n'th load step and i'th iteration loop.

Card 5

Columns	Quantity	Format
1-5	Load step intervals at which to print displacements (IPP1)	I5
6-10	Node ID for printing displacement (NPPP1)	I5
11-15	Degree of freedom ID for NPPP1 (NDDD1)	I5
16-20	Node ID for printing displacement (NPPP2)	I5
21-25	Degree of freedom ID for NPPP2 (NDDD2)	I5
26-30	Node ID for printing displacement (NPPP3)	I5
31-35	Degree of freedom IDfor NPPP3 (NDDD3)	I5
36-40	Node ID for printing energy release rate (NPPP4)	I5

The degree of freedom ID are 1 (*x*-displacement), 2 (*y*-displacement), 3 (*z*-displacement), 4 (*y*-rotation) and 5 (*x*-rotation). NPPP1, NPPP2 and NPPP3 are the node numbers where the displacements are printed out in the output file "*filename.path*". For example, NPPP1=273 and NDDD1=3, prints the *z*-displacement of node 273. NPPP4 is a node on the delamination front where the energy release rate is printed in the output file "*filename.zgm*".

Card 6

Columns	Quantity	Format
1-13	Elasticity modulus in fiber direction of lamina (E1)	E13.7
14-26	Elasticity modulus in transverse direction of lamina (E2)	E13.7
27-31	Poisson's ratio in plane 1-2 of lamina (PS1)	F5.2
32-36	Poisson's ratio in plane 2-1 of lamina (PS2)	F5.2
37-49	Shear modulus in plane 1-2 of lamina (G12)	E13.7
50-62	Shear modulus in plane 1-3 of lamina (G13)	E13.7
63-75	Shear modulus in plane 2-3 of lamina (G23)	E13.7

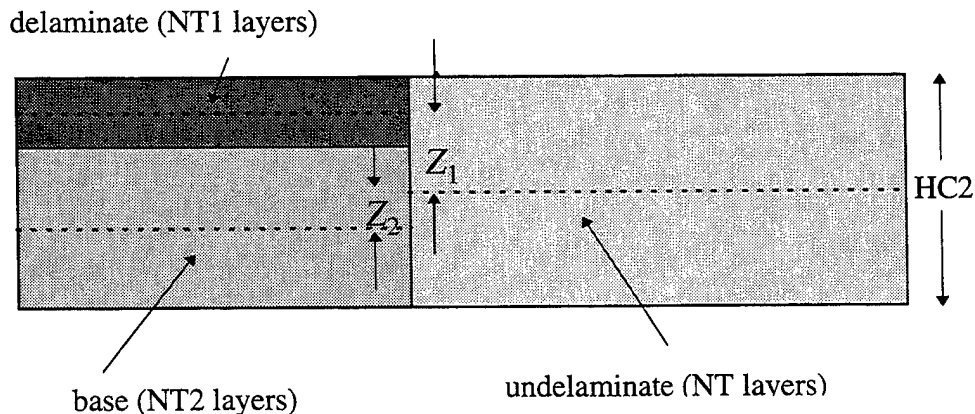
Card 7

Columns	Quantity	Format
1-12	Axial (extensional) rigidity of beam (EA)	E12.5
13-24	Bending rigidity of beam in the plane perpendicular to plate (EJ)	E12.5
25-36	Bending rigidity of beam in the plane parallel to plate (EJ1)	E12.5
37-48	Torsional rigidity of beam (GJ)	E12.5
49-60	Transverse shear rigidity of beam (GA)	E12.5
61-72	Feature not available, set to 0.0	E12.5
73-77	Eccentricity (ECCEN)	F5.2

ECCEN is the z -coordinate of the beam reference axis relative to the reference plane of the plate elements ($z = 0$).

Card 8

Columns	Quantity	Format
1-5	Number of plies in the undelaminate (NT)	I5
6-10	Number of plies in the delaminate (NT1)	I5
11-15	Number of plies in the the base (NT2)	I5
16-20	First undelaminate node on the delamination front if the delamination front intersects a boundary. If the delamination front does not intersect a boundary, any node on the undelaminate delamination front can be specified. (N11)	I5
21-25	Next undelaminate node on the delamination front in the CCW direction from node N11 (N22)	I5
26-35	Total laminate thickness (HC2)	F10.5
36-45	z-coordinate of mid-surface of delaminate with respect to undelaminate (Z_1)	F10.5
46-55	z-coordinate of mid-surface of base with respect to undelaminate (Z_2)	F10.5
56-65	Feature not available, set to 0.0 (AK1)	F10.5
66-75	Feature not available, set to 0.0 (AK2)	F10.5



Card 8+1 - Card 8+NT

Columns	Quantity	Format
1-10	Ply thickness (T)	F10.5
11-20	Ply angle (degrees) measured from the global x -axis (ZTA)	F10.5

These ply cards are written from the top of the laminate to the bottom (i.e. in the $+z$ to $-z$ direction).

Define the NUMNP nodes and the displacement and rotational boundary conditions in the next NUMNP cards.

Cards for Nodal Coordinates

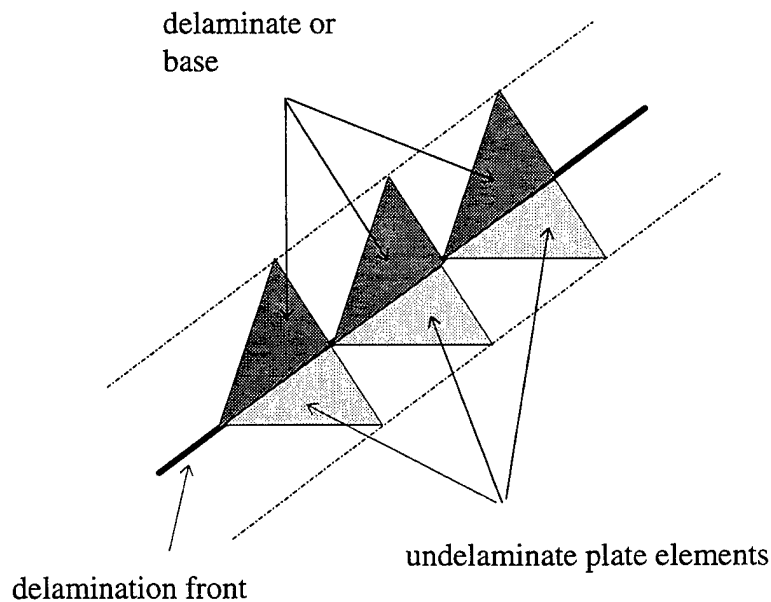
Columns	Quantity	Format
1-5	Node number	I5
6-10	Code for displacement boundary conditions = 0 no constraints = 1 x displacement is constrained = 2 y displacement is constrained = 3 z displacement is constrained = 4 x and y displacements are constrained = 5 y and z displacements are constrained = 6 x and z displacements are constrained = 7 x, y and z displacements are constrained	I5
11-30	x-coordinate	E20.10
31-50	y-coordinate	E20.10
51-70	z-coordinate	E20.10
71-75	Code for rotational boundary conditions = 0 no constraints = 1 x-axis rotation is constrained = 2 y-axis rotation is constrained = 4 x-axis and y-axis rotations are constrained	I5

Define the NEQ plate element connectivities and their locations in the next NEQ cards.

Cards for Plate Elements

Columns	Quantity	Format
1-5	Plate element number	I5
6-10	Location of plate element = 1 delaminate region = 2 base region = 3 undelaminate region	I5
11-15	node 1	I5
16-20	node 2	I5
21-25	node 3	I5

For plate elements on the delamination front, the delaminate or base elements on one side of the front and undelaminate elements on the other side, should be symmetric about the delamination front, as shown in the figure below. This restriction stems from the energy release rate calculation (see the Theory Manual for more information). If the user is not interested in the energy release rates, this requirement can be neglected.



Define the NEL beam element in the next NEL cards.

Cards for Beam Elements

Columns	Quantity	Format
1-5	Beam element number	I5
11-15	Node 1	I5
16-20	Node 2	I5

Define the JS0 concentrated (nodal) load cards.

Cards for Concentrated (Nodal) Loads

Columns	Quantity	Format
1-6	Node ID	I6
7-18	Force in the x -direction	F12.5
19-30	Force in the y -direction	F12.5
31-42	Force in the z -direction	F12.5
43-54	Moment in the x -direction	F12.5
55-66	Moment in the y -direction	F12.5

6 Output Files

The output file names are based on the name of the input file. The user is prompted for the input file name when BUCKDEL is executed. If the input file is "*filename.dat*", then the following set of output files are created.

filename.out: Echoes the main control variables, nodal coordinates, shell and beam element connectivities and material properties from the input file. The file contains information about nodes and elements on the delamination front. The linear solution due to reference load, buckling mode shape and buckling load are also available.

filename.femesh: The data in this file can be used to plot the finite element mesh of the model using GNUPlot.

filename.buck: The data in this file can be used to plot the fundamental buckling mode shape using GNUPlot.

filename.zg: The energy release rate at each node on the delamination front at each load step.

filename.zgm: The load factor (1st column), maximum energy release rate (2nd column) and the energy release rate at node NPPP4 (3rd column), at each load step.

filename.path: The load factor (1st column), displacements at nodes NPPP1 (2nd column), NPPP2 (3rd column), NPPP3 (4th column) at each load step.

filename.diff: Load factor and norm of the displacements along z-direction of nodes belonging to the base and undelaminate regions at each load step.

zmode.xx: z-displacements for plotting with GNUPlot at load step intervals specified by IPP1 (card 5, field 2). The extension "xx" is determined by the interval, IPP1. For example, if IPP1 is 4, then a sequence of files, "zmode.04", "zmode.08", "zmode.12",, etc., are created containing the z-displacements at the specified interval.

Files "*filename.zg*", "*filename.zgm*", "*filename.diff*" and "*filename.path*" are empty when the linear analysis options (IANALCD = 1 or 2) are specified.

To view the plot files "*filename.buck*" or "*zmode.xx*", execute GNUPlot and type the following at the prompt.

```
> set parametric off
> splot "filename.buck" w l
```

To view the finite element mesh in "*filename.femesh*", type the following at the prompt

```
> plot "filename.femesh" w l
```

GNUPlot can be used to create plots from the data files "*filename.path*" or "*filename.zgm*". For example, if it is desired to plot the displacement at node NPPP2 (column 3) vs. load factor (column 1) from data file "*filename.path*", type the following at the prompt,

```
> plot "filename.path" u 1:3 w l
```

Similarly, to plot the norm of the *z*-displacements of the base and undelaminate regions vs. load factor, type

```
> plot "filename.diff" u 1:2 w l
```

7 Example Problems

This section will illustrate some of the capabilities of BUCKDEL by solving several example problems. The input and output files for each example are distributed with the software so that the user can utilize them in learning how to run BUCKDEL.

7.1 Simply Supported Laminated Plate Under Biaxial Compression

A simply supported graphite-epoxy laminated plate under biaxial compression is shown in Figure 7-1. The loads per unit length in the *x* and *y* directions are λN_x and λN_y , respectively, with λ being the load factor. The lamina properties are: $E_1=18.5\text{e}+6$ psi, $E_2=1.89\text{e}+6$ psi, $G_{12}=0.93\text{e}+6$ psi, and $\nu_{12}=0.3$. The laminate has 16 plies with a ply thickness of 0.005 inches (total laminate thickness = 0.08 inches). The buckling load for several stacking sequences and values of N_y/N_x ($N_x=1.0$ psi) was computed with BUCKDEL. Due to symmetry, only one quarter of the plate was modeled with finite elements (see Figure 7-2). The results are shown in Table 7-1 where they are compared to those contained in [1]. In general, the agreement is very good. The slight differences are due to the fact that BUCKDEL accounts for shear deformation while the results from [1] do not. Figure 7-3 is a plot of the fundamental buckling mode ($N_y/N_x = 2.0$ case) produced by using GNUPlot to post-process the "*.buck" file created by BUCKDEL.

Table 7-1: Buckling loads for several stacking sequences and load ratios

N_y/N_x	Stacking Sequence	λ_{cr} (BUCKDEL)	λ_{cr} (Ref. [1])
0.2	$(45_3, -45_2, 90, 45_2, 90, -45)_s$	134.82	137.10
1.0	$(90, 45, 90_4, -45, 90)_s$	56.18	61.99
2.0	$(90_5, 45, -45, 90)_s$	35.68	36.84

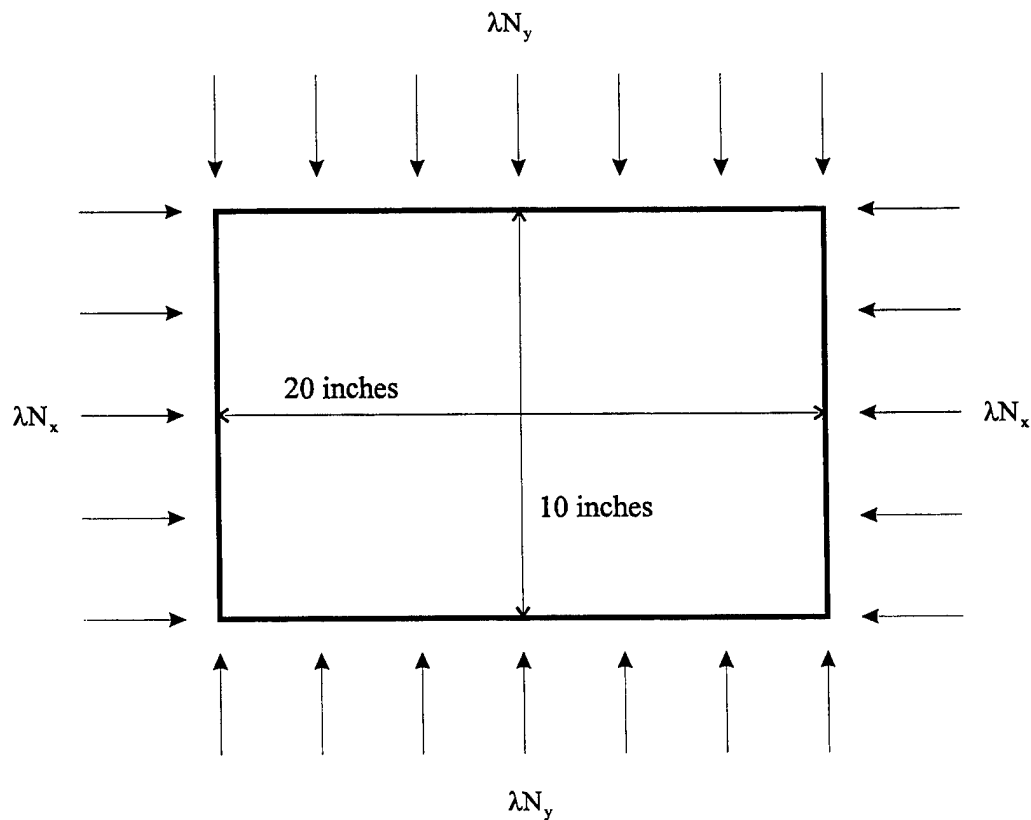


Figure 7-1: Simply supported graphite-epoxy laminated plate under biaxial compression

V1
L1
C1

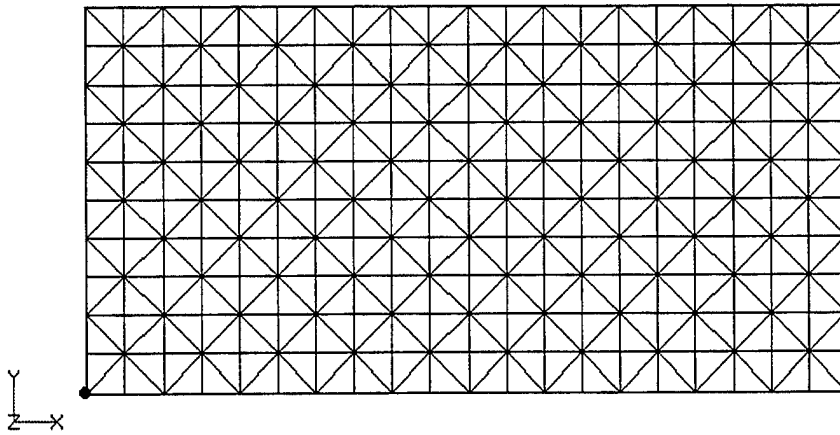


Figure 7-2: Finite element model of graphite-epoxy laminated plate

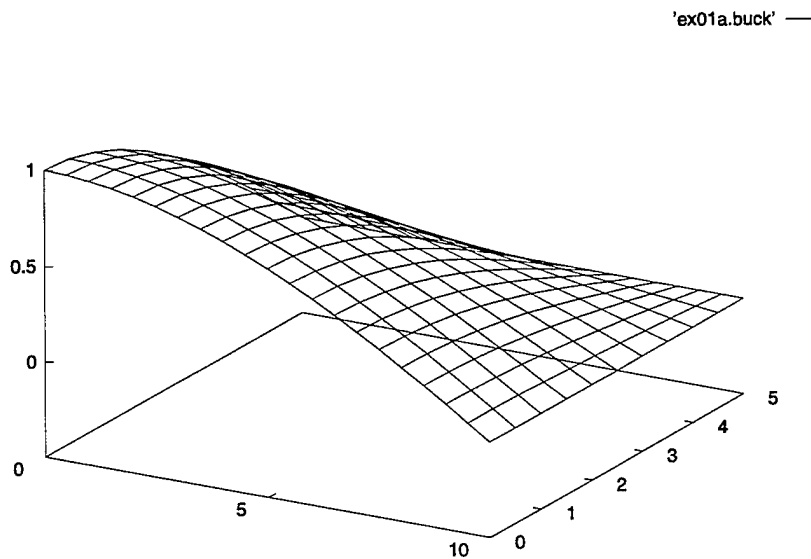


Figure 7-3: Fundamental buckling mode ($N_y/N_x = 2.0$ case)

7.2 Simply Supported Laminated Plate with Delamination

The simply supported graphite-epoxy laminated plate in Section 7.1 is reanalyzed, except that in this section a delamination is introduced. The lamina properties, geometry, etc. are the same as in Section 7.1. The delamination is centrally located in the plate. The load ratio is $N_y/N_x = 1.0$ and the ply stacking sequence is $(90, 45, 90_4, -45, 90)_s$. The analysis was performed with the delamination located at the mid-surface of the laminate (i.e. between the 90 plies) and between the 2nd and 3rd plies (45 and 90 plies) from the top face of the plate. The buckling load with the delamination at the mid-surface is 40.46

and the corresponding buckling mode can be seen in Figure 7-4, which was produced by using GNUPlot to post-process the "*.buck" file. When the delamination is located between the 2nd and 3rd plies, the buckling load is 15.09 and the buckling mode is plotted in Figure 7-5.

To demonstrate the difference between a "global" and "local" buckling mode (see the Theory Manual), it is useful to solve the same problem, except with the delamination replaced by a hole having the same dimensions as the delamination. If this is done, the buckling load is found to be 23.80 and the buckling mode is plotted in Figure 7-6. By comparing Figures 7-4, 7-5 and 7-6 one can observe that the buckling mode in Figure 7-5 is "local" while those in Figures 7-4 and 7-6 are "global". The importance in making this distinction is that if the user wants to investigate the effect of a delamination on the global buckling load, it is often necessary to perform a nonlinear post-buckling analysis. A linear buckling (eigenvalue) analysis of a structure with a delamination will often yield the "local" buckling load. The structure will still have a great deal of load carrying capability left after "local" buckling occurs. Thus, a design based on the "local" buckling load would be overly conservative.

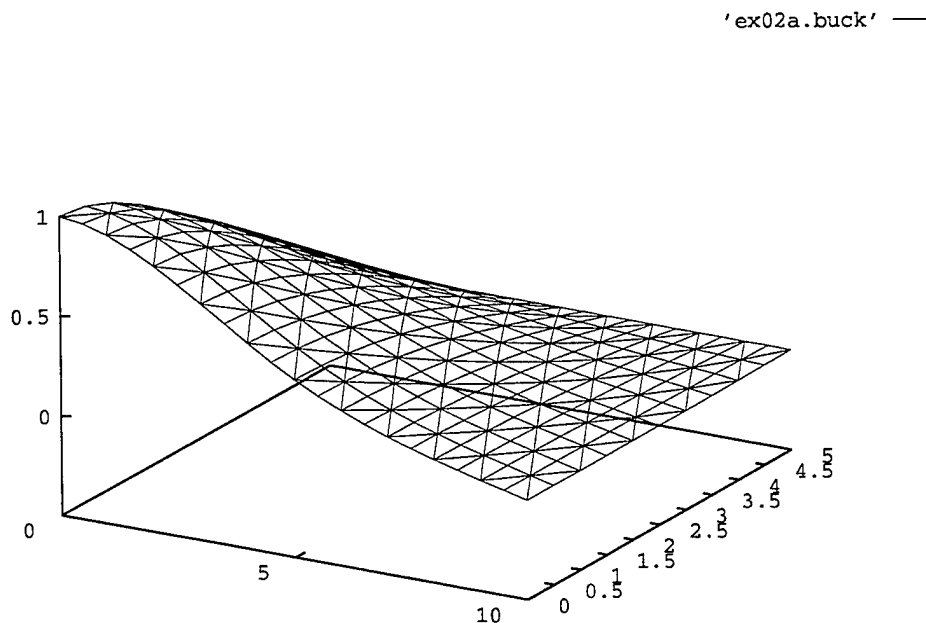


Figure 7-4: Fundamental buckling mode, delamination at mid-surface

'ex02b.buck' —

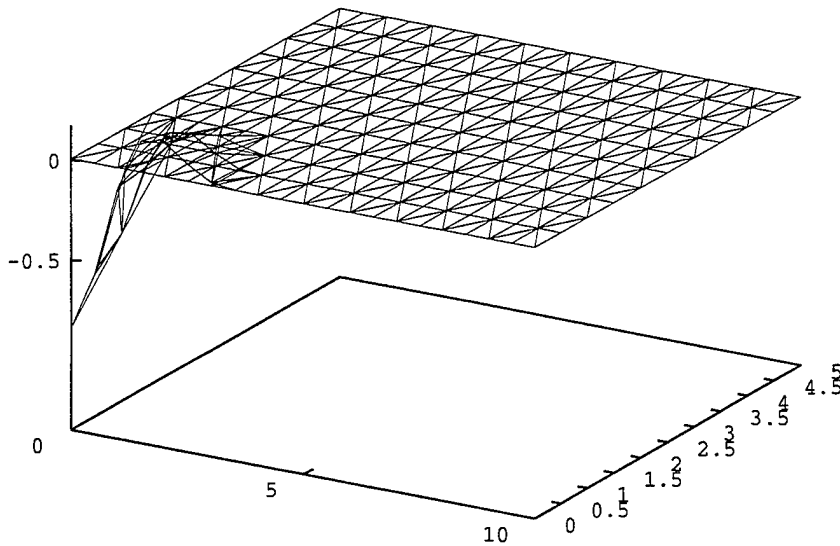


Figure 7-5: Fundamental buckling mode, delamination between 2nd and 3rd plies

'ex02c.buck' —

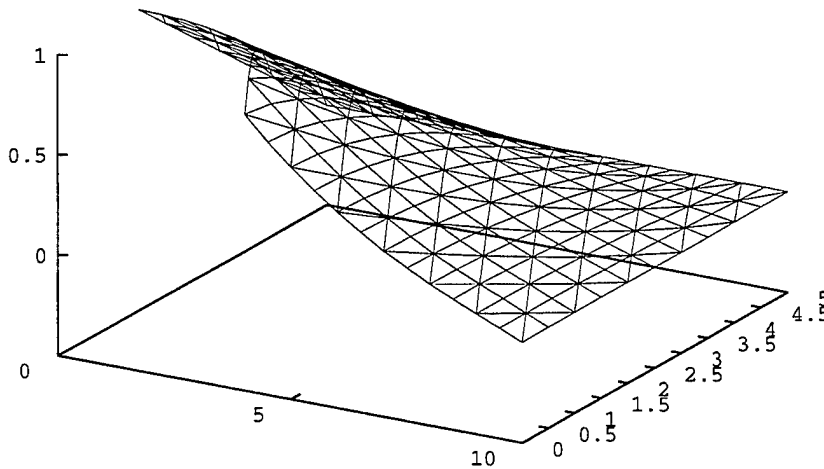


Figure 7-6: Fundamental buckling mode, plate with a hole

8 References

- [1] J.L. Walsh and R.T. Haftka; Stacking-Sequence Optimization for Buckling of Laminated Plates by Integer Programming, AIAA Journal, Vol. 30, No. 3, pp. 814-819, March 1992.

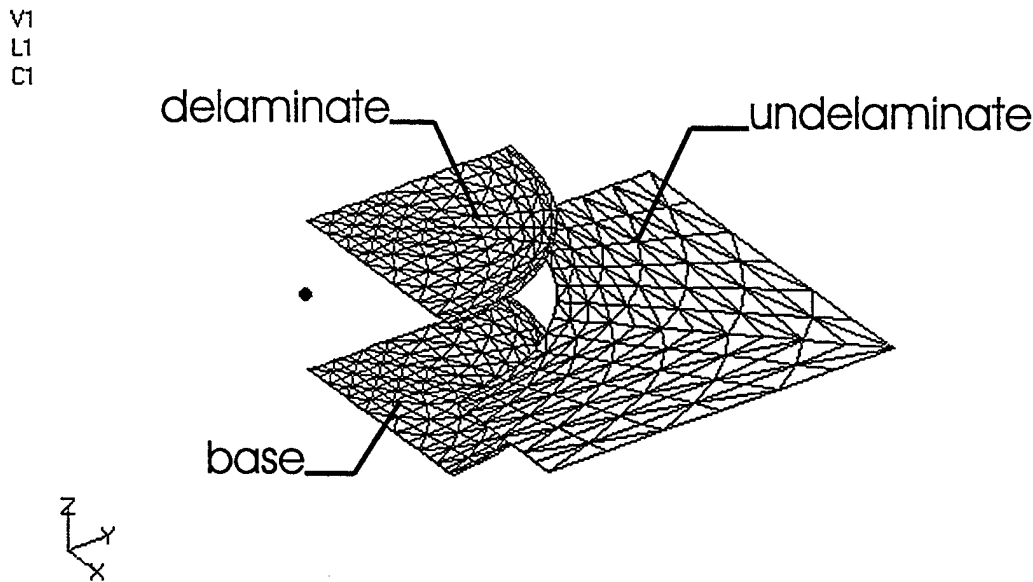


Figure 1: Multi-domain model of a laminated plate containing a delamination

1 INTRODUCTION

Laminated composites are gaining importance in aircraft structural applications due to their very high strength-to-weight ratios. These applications are, however, still very limited due in part to the lack of design tools capable of modeling the failure mechanisms involved in the laminated structures. BUCKDEL is a design tool which addresses this need. The BUCKDEL software performs geometrically nonlinear analysis of stiffened laminated composite shells with and without delaminations.

BUCKDEL allows the user to perform:

- a linear static solution;
- a linear buckling (eigenvalue) analysis; and
- a nonlinear post-buckling analysis through both limit and bifurcation points.

There are two finite elements implemented in BUCKDEL; a quasi-conforming triangular laminated shell element based on a refined first order shear theory with seven degrees of freedom per node and a fiber-reinforced beam element with seven degrees of freedom per node. The behavior of all materials is assumed to be linearly elastic.

The multi-domain modeling method is used for the analysis of laminated plates/shells containing delaminations. In this model, the delaminate, base and the undelaminate are modeled as 3 distinct plates (see Figure 1). On the delamination front, Mindlin's deformation assumption is applied to obtain the relationship between the displacements in the delaminate, base and undelaminate.

The remainder of this manual provides descriptions of the theoretical concepts associated with the BUCKDEL software. This begins with some basic concepts in damage

mechanics as it applies to laminated composite materials. Thereafter, a detailed description of the finite elements and solution schemes implemented in BUCKDEL are given.

2 DELAMINATIONS IN LAMINATED COMPOSITE MATERIALS

It is known that delaminations are the most frequent causes of failure of laminated structures, particularly under compressive loads. The presence of delaminations leads to a reduction in the overall buckling strength of the structure. In addition, the delaminations tend to grow rapidly under post-buckling loads, in particular, causing a further reduction in structural strength, and finally, leading to fatal structural failure.

Fiber reinforced Polymer Matrix Composites can, in general, be modeled as transversely isotropic linear elastic solids. Thus, each lamina in a laminated composite structure can be modeled as a transversely isotropic solid. However, when a laminate with an arbitrary (but perhaps *optimized*) stacking sequence of angle-ply lay-up is considered, additional couplings in the constitutive matrix result. In aircraft structures made up of PMC's, one can tailor the strength, stiffness, aeroelastic and acoustic response of the structure by optimizing the constituent properties as well as the stacking sequence. However, a stacking sequence that optimizes the stiffness and dynamic response may not necessarily be optimal from the point of view of controlling the deleterious interlaminar stresses which may induce local delaminations.

An obvious consequence of delamination on the bending behavior of a beam or plate is the complete absence of shear transfer from outer plies - carrying larger normal stress - to inner plies, except through friction when such tangential forces exist. However, more critical than the lack of the shear transfer, the composite laminate with delaminated areas may have local buckling phenomena in the presence of local compression loads when they exceed certain critical buckling loads at the ends of the delamination sites. Depending on the area and location of the delamination, the buckling may have different modes (Figure 2).

The global behavior of primary interest when designing aircraft structures made of PMC's is the buckling and post-buckling response of stiffened laminated composite plate and shell structures that contain reinforced or unreinforced cut-outs. Delaminations and local buckling may accompany and concurrently influence global buckling. The accurate prediction of the onset of local buckling due to delaminations and its effect on the global buckling and post-buckling response of a structure is essential in establishing the integrity of that structure. BUCKDEL provides a means of modeling the strength reduction due to the presence of the delaminations and the mechanisms of delamination growth. BUCKDEL can be used for modeling delaminated stiffened composite structures; for an accurate prediction of their geometrically nonlinear behavior under normal and post-buckling loading conditions; and for delamination growth prediction by using the pointwise energy release rate at the delamination front.

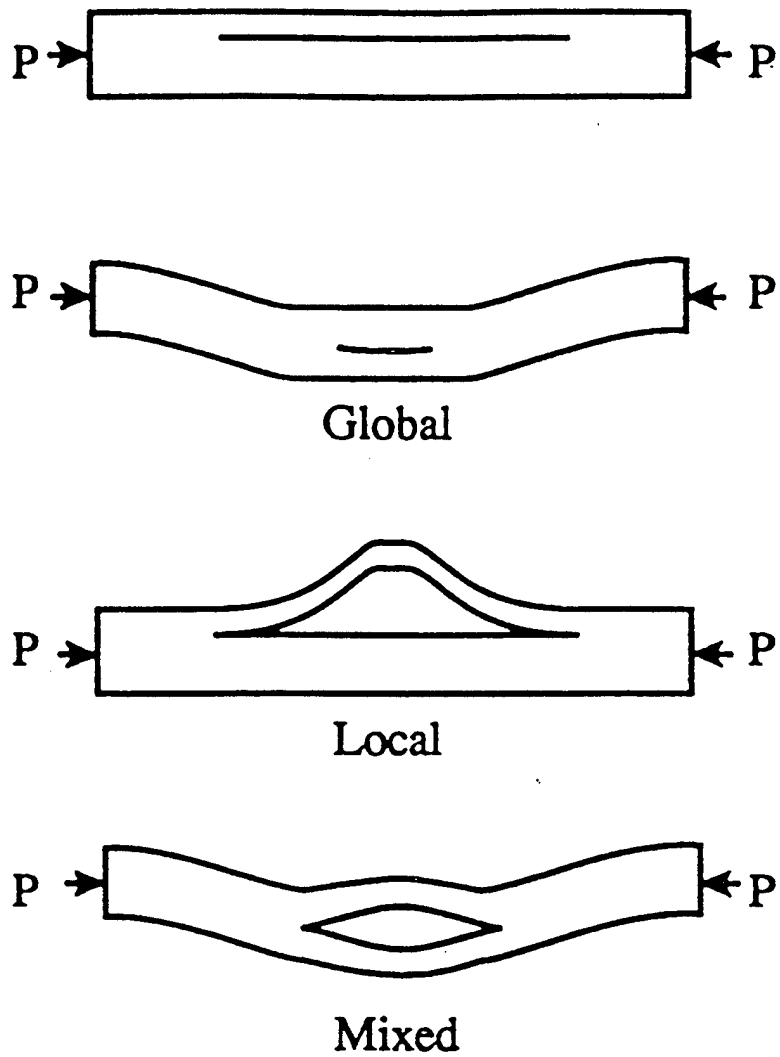


Figure 2: Buckling modes for a delaminated composite

3 MULTI-DOMAIN MODELING OF DELAMINATIONS

BUCKDEL can be used to analyze a general stiffened laminated composite plate/shell with a single delamination of an arbitrary shape and location, subjected to arbitrary compressive loads (Figure 3). The structure is modeled using the multi-domain model wherein the delaminated plate/shell is assumed to be assembled with three distinct plates or shells - (1) Laminate: nondelaminated zone $\Omega^{(1)}$; (2) Delaminate: thinner side of the delaminated zone $\Omega^{(2)}$ and (3) Base: thicker side of the delaminated zone $\Omega^{(3)}$. The three shells, $\Omega^{(i)}$, $i = 1, 2, 3$ respectively, have midsurface areas $\mathcal{A}^{(i)}$; thicknesses $t^{(i)}$; boundaries $\partial\Omega^{(i)}$; and midsurface boundaries $\partial\mathcal{A}^{(i)}$. The delamination edge is denoted by Γ . The assumptions of Reissner-Mindlin theory of plate bending are used for modeling each plate/shell and the joint between them. Thus, for each plate/shell, the 3-dimensional displacement field ($\mathbf{U} \equiv \{U_1 \ U_2 \ U_3\}$) can be expressed in terms of the corresponding midsurface displacement ($\mathbf{u} \equiv \{u_1 \ u_2 \ u_3\}$) and rotation ($\boldsymbol{\theta} \equiv \{\theta_1 \ \theta_2 \ 0\}$) fields as,

$$\mathbf{U}^{(i)}(x_\alpha, x_3) = \mathbf{u}^{(i)}(x_\alpha) - x_3^{(i)} \boldsymbol{\theta}^{(i)}(x_\alpha) \quad (1)$$

where $x_\alpha^{(i)}$ ($\alpha = 1, 2$) are the inplane curvilinear shell coordinates and $x_3^{(i)}$ is the thickness coordinate for the i^{th} ($i = 1, 2, 3$) shell (Figure 3). The structural continuity at the delamination front Γ is maintained by assuming the deformation to be unique at the junction of the three shells i.e. $\mathbf{U}^{(1)} = \mathbf{U}^{(2)} = \mathbf{U}^{(3)}$ on Γ in accordance with the Reissner-Mindlin law of flexure [equation (1)]. In other words, *at the delamination edge*, the mid-surface degrees of freedom of the delaminate and the base shells are assumed to be related to those of the nondelaminated shell by,

$$\begin{pmatrix} u_3^{(1)} & = & u_3^{(2)} & = & u_3^{(3)} \\ \theta_\alpha^{(1)} & = & \theta_\alpha^{(2)} & = & \theta_\alpha^{(3)} \\ u_\alpha^{(i)} & = & u_\alpha^{(1)} & + & h_\alpha^{(i)} \theta_\alpha^{(1)} \end{pmatrix}_{at \ \Gamma} \quad (2)$$

where $h^{(i)}$ is the distance of the midsurface of the i^{th} shell from the laminate midsurface (Figure 3). It can be noted that the above continuity conditions at the delamination edge can be modified appropriately when using any other alternative shell theory (e.g. higher order shear deformable theory) or by choosing appropriate heuristic multi-point constraints based on experience.

Similarly, the beam (stiffener) degrees of freedom are related to the shell degrees of freedom such that the transverse variations of deformation across the shell and beam section are consistent with Reissner-Mindlin theory:

$$\begin{aligned} u_3^b &= u_3^s \\ \theta_\alpha^b &= \theta_\alpha^s \\ u_\alpha^b &= u_\alpha^s + e \theta_\alpha^s \end{aligned} \quad (3)$$

where superscripts b and s represent beam and shell degrees of freedom respectively, and e is the eccentricity of the stiffener's neutral axis with reference to the neutral surface of the shell.

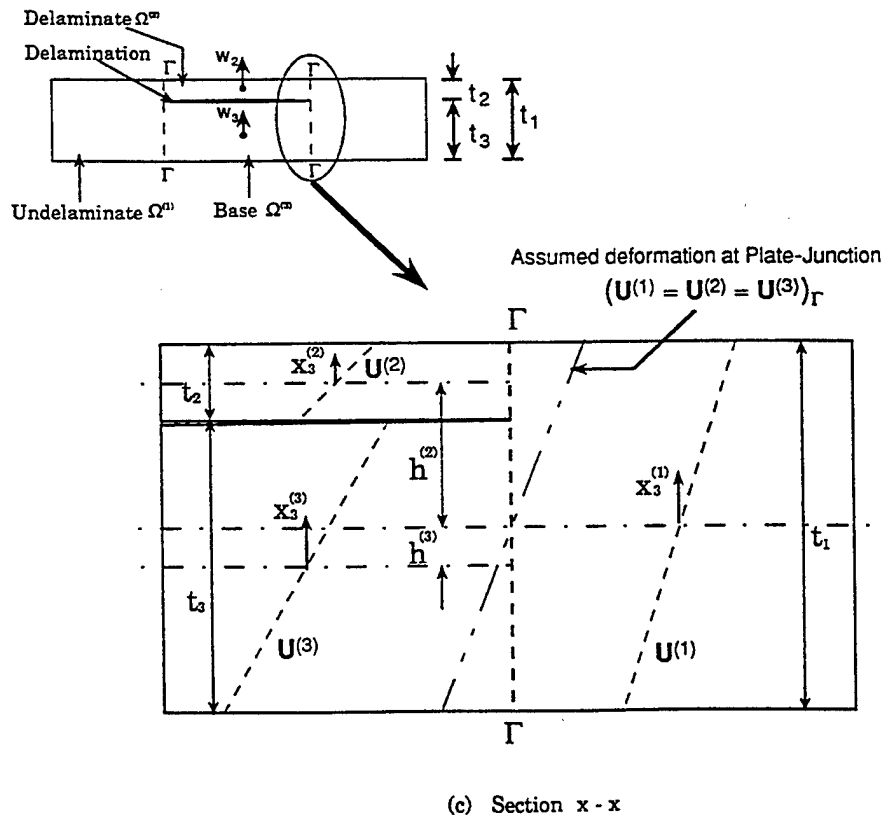
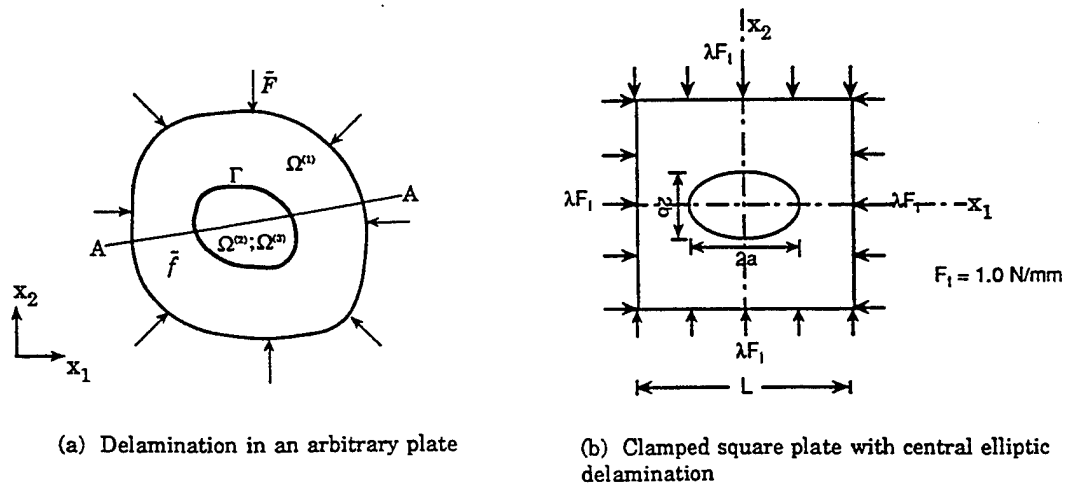


Figure 3: Multi-domain model

If ϕ_α ($\alpha = 1, 2$) are the *midsurface-rotations* characterizing the transformation of the normal to the undeformed mid-surface to that of the deformed mid-surface, we have,

$$\phi_\alpha = u_{3,\alpha} + b_{\alpha\beta}u_\beta \quad (4)$$

where \mathbf{b} is the curvature tensor of the shell's mid-surface.

In the present formulation, the engineering transverse shear strains $\gamma_{\alpha 3}$ are considered as independent mid-surface degrees of freedom, assuming that they do not vary over the shell thickness. The engineering transverse shear strains are related to the section rotations θ_α and the mid-surface rotations ϕ_α in accordance with the Reissner-Mindlin theory of plate flexure, as,

$$\gamma_{\alpha 3} = \phi_\alpha - \theta_\alpha \quad (5)$$

For each shell, the inplane strain components (ϵ_{11} , ϵ_{22} , ϵ_{12}) and the transverse shear strain components (ϵ_{13} , ϵ_{23}) of the 3-dimensional Green-Lagrange strain tensor (including large deformations) are given by,

$$\begin{aligned} \epsilon_{\alpha\beta}^{(i)} &= \frac{1}{2} [U_{\alpha,\beta} + U_{\beta,\alpha} + (U_{3,\alpha} + b_{\alpha\beta}U_\beta)(U_{3,\beta} + b_{\beta\alpha}U_\alpha) - b_{\alpha\beta}U_3]^{(i)} \\ \epsilon_{\alpha 3}^{(i)} &= \frac{1}{2} [\gamma_{\alpha 3}]^{(i)} \end{aligned} \quad (6)$$

respectively where, again, $\alpha, \beta = 1, 2$ and $i = 1, 2, 3$. Using the 3-dimensional displacement field description [equation (1)] in equations (6), and neglecting the nonlinear terms associated with the section rotations, the inplane components of the Green-Lagrange strain tensor can be simplified as,

$$\epsilon_{\alpha\beta}^{(i)} = (\epsilon_{\alpha\beta}^{(i)} + \nu_{\alpha\beta}^{(i)}) + x_3^{(i)} (\kappa_{\alpha\beta}^{(i)} + \chi_{\alpha\beta}^{(i)}) \quad (7)$$

where, $\epsilon_{\alpha\beta}^{(i)}$ and $\nu_{\alpha\beta}^{(i)}$ are the linear and nonlinear components of the membrane strains; and $\kappa_{\alpha\beta}^{(i)}$ and $\chi_{\alpha\beta}^{(i)}$ are the flexural strain components related to *mid-surface rotations* ϕ_α and transverse shear strains $\gamma_{\alpha 3}$ respectively, given by,

$$\begin{aligned} \epsilon_{\alpha\beta}^{(i)} &= \frac{1}{2} [u_{\alpha,\beta} + u_{\beta,\alpha}]^{(i)} - [b_{\alpha\beta}u_3]^{(i)} \\ \nu_{\alpha\beta}^{(i)} &= \frac{1}{2} [(u_{3,\alpha} + b_{\alpha\beta}u_\beta)(u_{3,\beta} + b_{\beta\alpha}u_\alpha)]^{(i)} \\ \kappa_{\alpha\beta}^{(i)} &= \frac{-1}{2} [(u_{3,\alpha} + b_{\alpha\beta}u_\beta)_{,\beta} + (u_{3,\beta} + b_{\beta\alpha}u_\alpha)_{,\alpha}]^{(i)} \\ \chi_{\alpha\beta}^{(i)} &= \frac{1}{2} [\gamma_{\alpha 3,\beta} + \gamma_{\beta 3,\alpha}]^{(i)} \end{aligned} \quad (8)$$

Equation (7) can be written in a compact form to express the 3-dimensional Green-Lagrange strain components $\epsilon^{(i)} = \{\epsilon_{11} \ \epsilon_{22} \ \epsilon_{12} \ \epsilon_{13} \ \epsilon_{23}\}^{(i)}$ in terms of the 2-dimensional strain components $\epsilon^{(i)} = \{\epsilon_{11} \ \epsilon_{22} \ \epsilon_{12}\}^{(i)}$; $\nu^{(i)} = \{\nu_{11} \ \nu_{22} \ \nu_{12}\}^{(i)}$; $\kappa^{(i)} = \{\kappa_{11} \ \kappa_{22} \ \kappa_{12}\}^{(i)}$; $\chi^{(i)} = \{\chi_{11} \ \chi_{22} \ \chi_{12}\}^{(i)}$ and $\gamma^{(i)} = \{\gamma_{13} \ \gamma_{23}\}^{(i)}$ as,

$$\epsilon^{(i)} = \left\{ (\epsilon + \nu) + x_3 \left(\kappa + \chi \right) \right\}^{(i)} = \mathbf{B} \cdot \delta \quad (9)$$

where $\delta = \{u_1 \ u_2 \ u_3 \ u_{3,1} \ u_{3,2} \ \gamma_{13} \ \gamma_{23}\}$ is the vector of independent degrees of freedom and \mathbf{B} is the strain-displacement matrix.

Assuming orthotropic material behavior for each lamina, the inplane stresses $\sigma^{(i)} = \{\sigma_{11} \ \sigma_{22} \ \sigma_{12}\}^{(i)}$ and the transverse shear stresses $\tau^{(i)} = \{\tau_{13} \ \tau_{23}\}^{(i)}$ are related to the corresponding strain components as,

$$\begin{Bmatrix} \sigma \\ \tau \end{Bmatrix}^{(i)} = \begin{bmatrix} E_{11} & E_{12} & E_{16} & 0 & 0 \\ E_{12} & E_{22} & E_{26} & 0 & 0 \\ E_{16} & E_{26} & E_{66} & 0 & 0 \\ 0 & 0 & 0 & E_{44} & E_{45} \\ 0 & 0 & 0 & E_{45} & E_{55} \end{bmatrix}^{(i)} \begin{Bmatrix} (\varepsilon + \nu) + x_3(\kappa + \chi) \\ \frac{1}{2}\gamma \end{Bmatrix}^{(i)} \quad (10)$$

where the material constitutive terms $E_{ij}^{(i)}$ are functions of the thickness coordinate of each shell $x_3^{(i)}$. Generally, for a laminate with orthotropic layers, $E_{ij}^{(i)}$ are assumed to be piecewise constants over the laminate thickness.

Now, for each shell, the strain energy density (per unit volume) can be calculated using equations (9) and (10) as,

$$W^{(i)} = [\sigma \cdot ((\varepsilon + \nu) + x_3(\kappa + \chi))]^{(i)} + [\tau \cdot \gamma]^{(i)} \quad (11)$$

As we can observe from equations (7) through (10), the strain field is a linear function in x_3 while the stress field is a piecewise linear function in x_3 . Hence, it is often more useful to integrate the strain energy density explicitly in the thickness direction and define strain energy density per unit area as,

$$\hat{W}^{(i)} = \int_{t_i} W^{(i)} dx_3 = [\mathbf{N} \cdot (\varepsilon + \nu) + \mathbf{M} \cdot (\kappa + \chi) + \mathbf{Q} \cdot \gamma]^{(i)} \quad (12)$$

where $\mathbf{N} \equiv \{N_{11} \ N_{22} \ N_{12}\}$ are the inplane stress resultants; $\mathbf{M} \equiv \{M_{11} \ M_{22} \ M_{12}\}$ are the bending moment resultants; and $\mathbf{Q} \equiv \{Q_{13} \ Q_{23}\}$ are the transverse shear stress resultants given, for each shell, by,

$$\begin{Bmatrix} \mathbf{N} \\ \mathbf{M} \\ \mathbf{Q} \end{Bmatrix}^{(i)} = \begin{bmatrix} \mathbf{A} & \mathbf{B} & \mathbf{0} \\ \mathbf{B} & \mathbf{D} & \mathbf{0} \\ \mathbf{0} & \mathbf{0} & \mathbf{G} \end{bmatrix}^{(i)} \begin{Bmatrix} (\varepsilon + \nu) \\ (\kappa + \chi) \\ \gamma \end{Bmatrix}^{(i)} \quad (13)$$

and

$$\begin{aligned} (A_{kl}; B_{kl}; D_{kl})^{(i)} &= \int_{t_i} E_{ij}^{(i)}(x_3) (1; x_3; x_3^2) dx_3 \\ G_{mn}^{(i)} &= \int_{t_i} s_m s_n E_{ij}^{(i)}(x_3) dx_3 \end{aligned}$$

as $k, l = 1, 2, 3$ correspond to $i, j = 1, 2, 6$ and $m, n = 1, 2$ correspond to $i, j = 4, 5$; and s_1 and s_2 are the shear correction factors in the transverse planes 1 – 3 and 2 – 3 respectively. Integrating $\hat{W}^{(i)}$ [equation (13)] over the shell domains we get the total strain energy stored in the i^{th} shell as,

$$\bar{W}^{(i)} = \frac{1}{2} \int_{\mathcal{A}^{(i)}} \hat{W}^{(i)} d\mathcal{A} = \int_{\mathcal{A}^{(i)}} \frac{1}{2} (\mathbf{N} \cdot (\varepsilon + \nu) + \mathbf{M} \cdot (\kappa + \chi) + \mathbf{Q} \cdot \gamma)^{(i)} d\mathcal{A} \quad (14)$$

If $\mathbf{f}^{(i)} = \{f_1 \ f_2 \ f_3\}^{(i)}$ are the body force components acting on the i^{th} shell; and $\mathbf{F} = \{F_1 \ F_2 \ F_3\}^{(i)}$ are the traction forces acting on the boundaries of the i^{th} shell - all defined in the curvilinear shell coordinate system - the potential of the external forces on the i^{th} shell is given by,

$$P^{(i)} = \int_{\Omega^{(i)}} \mathbf{f} \cdot \mathbf{U} \, d\Omega + \int_{\partial\Omega^{(i)}} \mathbf{F} \cdot \mathbf{U} \, d\mathcal{A} \quad (15)$$

Assuming that the body force components and the transverse traction force component do not vary over shell thickness and the inplane traction force components vary linearly over the thickness, we get,

$$P^{(i)} = \int_{\mathcal{A}^{(i)}} (\hat{\mathbf{f}} \cdot \mathbf{u})^{(i)} \, d\mathcal{A} + \int_{\partial\mathcal{A}^{(i)}} (\hat{\mathbf{F}} \cdot \mathbf{u} + \hat{\mathbf{M}} \cdot \boldsymbol{\theta})^{(i)} \, d\Gamma \quad (16)$$

where,

$$\hat{\mathbf{f}}^{(i)} = \int_{t_i} \mathbf{f}^{(i)} dx_3 \quad ; \quad \hat{\mathbf{F}}^{(i)} = \int_{t_i} \mathbf{F}^{(i)} dx_3 \quad ; \quad \hat{\mathbf{M}}^{(i)} = \int_{t_i} \mathbf{F}^{(i)} x_3 dx_3$$

and $\hat{\mathbf{M}}^{(i)} = \{\hat{M}_1 \ \hat{M}_2 \ 0\}^{(i)}$ represent the traction moments acting on $\partial\mathcal{A}^{(i)}$.

Then, using equations (14) and (15), the total potential energy for the assembly of shells is given by,

$$\Pi = \sum_{i=1}^3 (\bar{W}^{(i)} - P^{(i)}) \quad (17)$$

Applying the minimum total potential energy principle ($\delta\Pi = 0$), we obtain the following internal equilibrium equations for each shell,

$$\begin{pmatrix} (N_{\alpha\beta} + b_{\alpha\eta} M_{\eta\beta})_{,\beta} - b_{\alpha\eta} N_{\eta\beta} \phi_{\beta} + \hat{f}_{\alpha} & = & 0 \\ M_{\alpha\beta,\beta} + Q_{\alpha 3} & = & 0 \\ (Q_{\alpha 3} + N_{\alpha\beta} (u_{3,\beta} + b_{\beta\eta} u_{\eta}))_{,\alpha} + \hat{f}_3 & = & 0 \end{pmatrix}_{\mathcal{A}^{(i)}} \quad (18)$$

and the following boundary conditions on the external boundary of each shell,

$$\left(\begin{array}{lll} u_{\alpha} & = & 0 \quad or \\ u_{3,\alpha} + b_{\alpha\eta} u_{\eta} - \gamma_{\alpha 3} & = & 0 \quad or \\ u_3 & = & 0 \quad or \end{array} \quad \begin{array}{l} N_{\alpha\beta} n_{\beta} = \hat{F}_{\alpha} \\ M_{\alpha\beta} n_{\beta} = \hat{M}_{\alpha} \\ (Q_{\alpha 3} + N_{\alpha\beta} (u_{3,\beta} + b_{\beta\eta} u_{\eta})) n_{\alpha} = \hat{F}_3 \end{array} \right)_{\partial\mathcal{A}^{(i)}} \quad (19)$$

where n_i is the i^{th} component of the unit vector \mathbf{n} normal to delamination front. The displacement is continuous at the delamination edge and therefore, on Γ we have:

$$(\delta\mathbf{U}^{(1)} = \delta\mathbf{U}^{(2)} = \delta\mathbf{U}^{(3)})_{\Gamma} \quad (20)$$

Hence, for equilibrium, the following conditions have to be satisfied at any point on the delamination edge:

$$\{\mathcal{F}_n(\mathbf{N}) = 0 \quad ; \quad \mathcal{F}_n(\mathbf{M}') = 0 \quad ; \quad \mathcal{F}_n(\mathbf{T}) = 0\}_{\Gamma} \quad (21)$$

where $\mathcal{F}_n(*) = (*)^{(1)} - (*)^{(2)} - (*)^{(3)}$ with $(*)^{(i)}$ corresponding to the value of $(*)$ at the specified point on the delamination boundary of the i^{th} shell; $(\mathbf{M}')^{(i)} =$

$\mathbf{M}^{(i)} + h^{(i)}\mathbf{N}^{(i)}$; and $T_\alpha = Q_{\alpha 3} + N_{\alpha\beta}(u_{3,\beta} + b_{\beta\eta}u_\eta)$ is the effective shear force. It can be noted that these conditions are normally satisfied in a finite element model. However, conflict may arise if the delamination edge touches the structural boundary, particularly the boundary with specified displacements where the stresses are expected to develop. Since the delamination generally acts as an imperfection, it is often possible that the base can come in contact with the delaminate after global buckling sets in, and then the above equilibrium equations (21) may not be valid. Thus the model can be effectively used for examining the growth of embedded delaminations under post-buckling conditions as long as the delaminated plies do not come in contact with each other.

4 FINITE ELEMENT FORMULATIONS

A 2-noded curved beam element (BEAM2) and a 3-noded shell element (SHELL3) are used by BUCKDEL for modeling stiffened shells. The transverse shear deformation is introduced explicitly in accordance with the Reissner-Mindlin plate theory. Reduced integration is used for the constrained membrane strain energy component to eliminate locking from the elements. The beam degrees of freedom are related to the corresponding shell degrees of freedom in accordance with the Reissner-Mindlin theory of flexure.

4.1 BEAM2: 2-noded curved beam element

The element incorporates the following independent degrees of freedom: u - inplane displacement; w - transverse displacement; $w_{,x}$ - slope of midsurface deflection and γ - the transverse shear strain. Thus the element requires C^0 -continuous fields for u and γ , and C^1 -continuous field for w . Linear Lagrangian polynomials are used for geometric description x and for the inplane displacement component u :

$$x = h_1 + h_2\xi \quad (22)$$

$$u = \alpha_1 + \alpha_2\xi \quad (23)$$

and cubic Hermitian polynomials are used for the transverse deflection w :

$$w = \beta_1 + \beta_2\xi + \beta_3\xi^2 + \beta_4\xi^3 \quad (24)$$

where ξ is the natural coordinate; and h_i , α_i and β_i are functions of nodal values x_i , u_i and w_i respectively.

4.2 SHELL3: 3-noded triangular curved shell element

The element is described in the curvilinear coordinate system $x - y$ and the area coordinates are used for field-description. Accordingly we have,

$$\{x \ y \ 1\} = \sum_{i=1}^3 L_i \{x \ y \ 1\}_i \quad (25)$$

Inverting the above relationship, we get,

$$L_i = \frac{1}{2\Delta} (a_{i1}x + a_{i2}y + a_{i3}) \quad (26)$$

where

$$\begin{aligned} a_{i1} &= y_j - y_k; \quad a_{i2} = x_k - x_j; \quad a_{i3} = x_j y_k - x_k y_j \\ \Delta &= \frac{1}{2} (x_2 y_3 - x_3 y_2 + x_3 y_1 - x_1 y_3 + x_1 y_2 - x_2 y_1) \end{aligned}$$

and $j = 2, 3, 1$; $k = 3, 1, 2$ as $i = 1, 2, 3$.

The inplane displacements and the transverse shear strains need to satisfy C^0 - continuity while the transverse deflection need to satisfy C^1 -continuity in the present formulation. The independent field variables u , v , w , γ_{xz} and γ_{yz} are expressed in terms of the nodal degrees of freedom u_i , v_i , w_i , $\varrho_{x_i} \equiv (-w,_{,y})_i$, $\varrho_{y_i} \equiv (w,_{,x})_i$, γ_{xz_i} and γ_{yz_i} as,

$$\begin{aligned} \{u \ v \ \gamma_{xz} \ \gamma_{yz}\} &= \sum_{i=1}^3 L_i \{u \ v \ \gamma_{xz} \ \gamma_{yz}\}_i \\ w &= \sum_{i=1}^3 (N_{1i} w_i + N_{2i} \varrho_{x_i} + N_{3i} \varrho_{y_i}) \end{aligned} \quad (27)$$

where,

$$\begin{aligned} N_{1i} &= L_i + L_i^2 L_j + L_i^2 L_k - L_i L_j^2 - L_i L_k^2 \\ N_{2i} &= a_{k1} \left(L_i^2 L_j + \frac{1}{2} L_i L_j L_k \right) + a_{j1} \left(L_i^2 L_k + \frac{1}{2} L_i L_j L_k \right) \\ N_{3i} &= a_{k2} \left(L_i^2 L_j + \frac{1}{2} L_i L_j L_k \right) + a_{j2} \left(L_i^2 L_k + \frac{1}{2} L_i L_j L_k \right) \end{aligned} \quad (28)$$

are the cubic polynomials for the transverse deflection.

The quasi-conforming shell element (Atluri, Huang and Shenoy [1]) is developed from the Hu-Washizu variational principle as follows. If the inter-element C^0 continuity is satisfied a priori, the Hu-Washizu principle can be written simply as the sum of the respective integrals for each of the finite elements (Atluri [2]), as:

$$\begin{aligned} \delta \sum_m \left(\int_{\Omega_m} \left\{ A(\epsilon) + \sigma : \left[\frac{1}{2} (\nabla \mathbf{u} + \mathbf{u} \nabla + \nabla \mathbf{u} \cdot \mathbf{u} \nabla) - \epsilon \right] - \mathbf{f}^o \cdot \mathbf{u} \right\} dV \right. \\ \left. - \int_{S_{\sigma m}} \mathbf{t}^o \cdot \mathbf{u} dA + \int_{S_{um}} \mathbf{n} \cdot \sigma \cdot (\mathbf{u} - \mathbf{u}^o) dA \right) = 0 \end{aligned} \quad (29)$$

where σ and ϵ are respectively the second Piola-Kirchhoff stress tensor and Green strain tensor, S_{um} and $S_{\sigma m}$ are the segments of the boundary of element m where displacements and tractions are prescribed respectively. If $\mathbf{u} = \mathbf{u}^o$ on S_{um} , and σ is considered as a Lagrange multiplier, Eq. (29) may be cast into the following *conditional* two-field variational problem

$$\delta \sum_m \left(\int_{\Omega_m} \{ A(\epsilon) - \mathbf{f}^o \cdot \mathbf{u} \} dV - \int_{S_{\sigma m}} \mathbf{t}^o \cdot \mathbf{u} dA \right) = 0 \quad (30)$$

$$\frac{1}{2} (\nabla \mathbf{u} + \mathbf{u} \nabla + \nabla \mathbf{u} \cdot \mathbf{u} \nabla) - \epsilon = \mathbf{0} \quad (m = 1, 2, \dots, N) \quad (31)$$

for all element strain and displacement fields, where N is the number of elements. The constraint condition in Eq. (31) may now be satisfied in a weak form if the independently assumed strain fields ϵ are expressed in terms of the element displacement fields through the element-level "quasi-conforming" condition:

$$\int_{\Omega_m} \delta \sigma : \left[\frac{1}{2} (\nabla \mathbf{u} + \mathbf{u} \nabla + \nabla \mathbf{u} \cdot \mathbf{u} \nabla) - \epsilon \right] dV = 0 \quad (m = 1, 2, \dots, N), \quad (32)$$

$\delta \sigma$ is an independent test-function for each element. When the element strain fields ϵ are expressed in terms of element displacement fields through Eq. (32), the two-field problem reduces to a one-field variational problem:

$$\delta \sum_m \left(\int_{\Omega_m} \{A(\epsilon(\mathbf{u})) - \mathbf{f}^o \cdot \mathbf{u}\} dV - \int_{S_{\sigma m}} \mathbf{t}^o \cdot \mathbf{u} dA \right) = 0 \quad (33)$$

$$\mathbf{u} = \mathbf{u}^o \text{ on } S_{um}$$

The strain energy of the laminated composite shell element can be expressed in the form

$$\int_{\Omega_m} A(\epsilon) dV = \frac{1}{2} \int_{A_m} (N^{\alpha\beta} \epsilon_{\alpha\beta o} + M^{\alpha\beta} \kappa_{\alpha\beta} + Q^\alpha \gamma_{\alpha\beta}) dA, \quad (34)$$

where A_m is the area of the element.

Since $\delta \sigma$ in Eq. (32) is a continuously differentiable, but otherwise arbitrary, test function that varies in the three co-ordinates x^i of the shell space, we assume a specific form for such a test function, denoted by ϵ^* , possessing a linear variation in the thickness direction x^3 . We thus have

$$\epsilon^* = (\epsilon^{*\alpha\beta} + x^3 \kappa^{*\alpha\beta}) \mathbf{a}_\alpha \mathbf{a}_\beta + \epsilon^{*\alpha 3} \mathbf{a}_\alpha \mathbf{a}_3. \quad (35)$$

Using Eq. (35) in Eq. (32) and integrating through x^3 , we obtain

$$\begin{aligned} & h \int_{A_m} \epsilon^{*\alpha\beta} \left\{ \frac{1}{2} [(u_{\alpha;\beta} + u_{\beta;\alpha}) - 2b_{\alpha\beta} w + (w_{,\alpha} + b_\alpha^\mu u_\mu)(w_{,\beta} + b_\beta^\mu u_\mu) - \epsilon_{\alpha\beta o}] \right\} dA \\ & + \frac{h^3}{12} \int_{A_m} \kappa^{*\alpha\beta} \left\{ -\frac{1}{2} [(w_{,\alpha} + b_\alpha^\mu u_\mu)_{;\beta} + (w_{,\beta} + b_\beta^\mu u_\mu)_{;\alpha} - \gamma_{\alpha 3;\beta} - \gamma_{\beta 3;\alpha}] - \kappa_{\alpha\beta} \right\} dA \\ & + h \int_{A_m} \epsilon^{*\alpha 3} (w_{,\alpha} + b_\alpha^\mu u_\mu - \theta_\alpha - \gamma_{\alpha 3}) dA = 0. \end{aligned} \quad (36)$$

Furthermore, $\epsilon_{\alpha\beta o}$ and $\kappa_{\alpha\beta}$ can be divided into two parts, respectively as

$$\epsilon_{\alpha\beta o} = \epsilon_{\alpha\beta o}^{(1)} + \epsilon_{\alpha\beta o}^{(2)} \quad (37)$$

$$\kappa_{\alpha\beta} = \kappa_{\alpha\beta}' + \kappa_{\alpha\beta}'', \quad (38)$$

where $\epsilon_{\alpha\beta o}^{(1)}$ are the components of the linear strain tensor, $\kappa'_{\alpha\beta}$ is the total curvature change of the middle-surface,

$$\epsilon_{\alpha\beta o}^{(1)} = \frac{1}{2}(u_{\alpha;\beta} + u_{\beta;\alpha}) - b_{\alpha\beta}w \quad (39)$$

$$\kappa'_{\alpha\beta} = -\frac{1}{2}[(w_{,\alpha} + b_{\alpha}^{\mu}u_{\mu})_{;\beta} + (w_{,\beta} + b_{\beta}^{\mu}u_{\mu})_{;\alpha}], \quad (40)$$

and $\epsilon_{\alpha\beta o}^{(2)}$ and $\kappa''_{\alpha\beta}$ denote the non-linear terms of the in-plane strain tensor, and curvature change due to transverse shear alone, respectively:

$$\epsilon_{\alpha\beta o}^{(2)} = \frac{1}{2}\phi_{\alpha}\phi_{\beta} \quad (41)$$

$$\kappa''_{\alpha\beta} = \frac{1}{2}(\gamma_{\alpha 3;\beta} + \gamma_{\beta 3;\alpha}) \quad (42)$$

If Eq. (42) are satisfied a priori, sufficient conditions for the satisfaction of Eq. (36) follow

$$\begin{aligned} & \int_{A_m} \epsilon^{*\alpha\beta} \left\{ \frac{1}{2}(u_{\alpha;\beta} + u_{\beta;\alpha} - 2b_{\alpha\beta}w) - \epsilon_{\alpha\beta o}^{(1)} \right\} dA \\ & + \int_{A_m} \epsilon^{*\alpha\beta} \left\{ \frac{1}{2}[(w_{,\alpha} + b_{\alpha}^{\mu}u_{\mu})(w_{,\beta} + b_{\beta}^{\mu}u_{\mu})] - \frac{1}{2}\phi_{\alpha}\phi_{\beta} \right\} dA = 0 \end{aligned} \quad (43)$$

$$\int_{A_m} \kappa^{*\alpha\beta} \left\{ \frac{1}{2}[(w_{,\alpha} + b_{\alpha}^{\mu}u_{\mu})_{;\beta} + (w_{,\beta} + b_{\beta}^{\mu}u_{\mu})_{;\alpha}] - \kappa'_{\alpha\beta} \right\} dA = 0 \quad (44)$$

$$\int_{A_m} \phi^{*\alpha} \{(w_{,\alpha} + b_{\alpha}^{\mu}u_{\mu}) - \phi_{\alpha}\} dA = 0, \quad (45)$$

where the notation ϵ^{*a3} is replaced by $\phi^{*\alpha}$. When Eq. (45) is satisfied for a complete family of test functions or the areas A_m are infinitesimal, we have

$$(w_{,\alpha} + b_{\alpha}^{\mu}u_{\mu}) - \phi_{\alpha} = 0.$$

Thus Eq. (43) reduces approximately to

$$\int_{A_m} \epsilon^{*\alpha\beta} \left\{ \frac{1}{2}(u_{\alpha;\beta} + u_{\beta;\alpha} - 2b_{\alpha\beta}w) - \epsilon_{\alpha\beta o}^{(1)} \right\} dA = 0; \quad (46)$$

when Eq. (45) is satisfied for a cut-off family of test functions (including a constant one) and the areas A_m are sufficiently small.

The Eqs. (46), (44) and (45), as the “quasi-conforming” conditions, are used to determine the undetermined parameters of $\epsilon_{\alpha\beta o}^{(1)}$, $\kappa'_{\alpha\beta}$, ϕ_{α} in terms of the displacement parameters, which are subsequently substituted into Eq. (33).

In the quasi-conforming element, the linear part of strains $\epsilon_{\alpha\beta o}^{(1)}$, the total curvature change of the middle surface $\kappa'_{\alpha\beta}$ and rotations ϕ_{α} in Eq. (33) are discretized directly

and the undetermined parameters in them are expressed in terms of the displacement field, viz. the generalized displacements at the nodes. In addition, the transverse shear strains $\gamma_{\alpha 3}$ in Eq. (33) are discretized by means of their values at the nodes. Based on a Lagrangean description, using Eq. (33), the formulation of the incremental equilibrium equations in terms of the generalized displacements is now presented.

Let $(\lambda_i, \mathbf{u}_i)$ denote a point (i) on the equilibrium path, $(\lambda_{i+1}, \mathbf{u}_{i+1})$ is a required point $(i+1)$

$$\mathbf{u}_{i+1} = \mathbf{u}_i + \Delta \mathbf{u}_i \quad (47)$$

$$\lambda_{i+1} = \lambda_i + \Delta \lambda_i$$

where λ is the load factor.

Substituting Eqs.(37, 38) into the constitutive relation for the composite laminate, we have

$$\begin{Bmatrix} \mathbf{N} \\ \mathbf{M} \end{Bmatrix} = \begin{Bmatrix} \mathbf{N}^{(1)} \\ \mathbf{M}^{(1)} \end{Bmatrix} + \begin{Bmatrix} \mathbf{N}^{(2)} \\ \mathbf{M}^{(2)} \end{Bmatrix} \quad (48)$$

where

$$\left(\begin{Bmatrix} \mathbf{N}^{(1)} \\ \mathbf{M}^{(1)} \end{Bmatrix}, \begin{Bmatrix} \mathbf{N}^{(2)} \\ \mathbf{M}^{(2)} \end{Bmatrix} \right) = \begin{bmatrix} \mathbf{A} & \mathbf{B} \\ \mathbf{B} & \mathbf{D} \end{bmatrix} \left(\begin{Bmatrix} \epsilon_o^{(1)} \\ \kappa \end{Bmatrix}, \begin{Bmatrix} \epsilon_o^{(2)} \\ \mathbf{0} \end{Bmatrix} \right) \quad (49)$$

and \mathbf{N} and \mathbf{M} are the stress resultants and couples and the terms \mathbf{A} , \mathbf{B} , and \mathbf{D} involve the laminate material constants.

Let $\boldsymbol{\eta}$ and $\Delta \boldsymbol{\eta}$ denote the generalized nodal displacements corresponding to the displacements \mathbf{u} and $\Delta \mathbf{u}$ and define the matrices \mathbf{K}_0 , \mathbf{K}_1 and \mathbf{K}_2 as follows

$$\begin{aligned} \delta \boldsymbol{\eta}^T \mathbf{K}_0 \boldsymbol{\eta} &= \sum_m \int_{A_m} \left\{ \mathbf{N}^{(1)T}(\mathbf{u}) \epsilon_o^{(1)}(\delta \mathbf{u}) + \mathbf{M}^{(1)T}(\mathbf{u}) \kappa(\delta \mathbf{u}) \right. \\ &\quad \left. + \mathbf{Q}^T(\mathbf{u}) \gamma(\delta \mathbf{u}) \right\} dA \end{aligned} \quad (50)$$

$$\begin{aligned} \delta \boldsymbol{\eta}^T \mathbf{K}_1(\boldsymbol{\eta}', \boldsymbol{\eta}'') \boldsymbol{\eta} &= \sum_m \int_{A_m} \left\{ 2 \left(\mathbf{N}^{(1)T}(\mathbf{u}'') + 2 \mathbf{N}^{(11)T}(\mathbf{u}', \mathbf{u}'') + \mathbf{N}^{(2)T}(\mathbf{u}'') \right) \epsilon_o^{(11)}(\mathbf{u}, \delta \mathbf{u}) \right. \\ &\quad \left. + 2 \mathbf{N}^{(1)T}(\delta \mathbf{u}) \epsilon_o^{(11)}(\mathbf{u}'', \mathbf{u}) + 2 \mathbf{N}^{(1)T} \epsilon_o^{(11)}(\mathbf{u}'', \delta \mathbf{u}) \right\} dA \end{aligned} \quad (51)$$

$$\begin{aligned} \delta \boldsymbol{\eta}^T \mathbf{K}_2(\boldsymbol{\eta}', \boldsymbol{\eta}'') \boldsymbol{\eta} &= \sum_m \int_{A_m} \left\{ 2 \mathbf{N}^{(11)T}(\delta \mathbf{u}, \mathbf{u}') \epsilon_o^{(11)}(\mathbf{u}'', \mathbf{u}) \right. \\ &\quad \left. + 2 \mathbf{N}^{(11)T}(\delta \mathbf{u}, \mathbf{u}'') \epsilon_o^{(11)}(\mathbf{u}', \delta \mathbf{u}') \right\} dA \end{aligned} \quad (52)$$

in which \mathbf{u}' and \mathbf{u}'' are allowed to assume $\mathbf{0}$, \mathbf{u}_i and $\Delta \mathbf{u}_i$, similarly $\boldsymbol{\eta}'$ and $\boldsymbol{\eta}''$ may assume $\mathbf{0}$, $\boldsymbol{\eta}_i$ and $\Delta \boldsymbol{\eta}_i$, and the symmetric bilinear forms $\epsilon_o^{(11)}$ and $\mathbf{N}^{(11)}$ are defined by

$$\epsilon_o^{(11)}(\mathbf{u}', \mathbf{u}'') = \frac{1}{2} [\phi_1(\mathbf{u}') \phi_1(\mathbf{u}''), \phi_2(\mathbf{u}') \phi_2(\mathbf{u}''), \phi_1(\mathbf{u}') \phi_2(\mathbf{u}'') + \phi_1(\mathbf{u}'') \phi_2(\mathbf{u}')]^T \quad (53)$$

$$\mathbf{N}^{(11)} = \mathbf{A} \epsilon_o^{(11)}.$$

Using the above definitions in equations Eq. (33) and Eq. (34), retaining all the non-linear terms, we obtain the equilibrium equations

$$\left[\mathbf{K}_0 + \mathbf{K}_1(\mathbf{0}, \boldsymbol{\eta}_i) + \mathbf{K}_2(\boldsymbol{\eta}_i, \boldsymbol{\eta}_i) + \frac{1}{2}\mathbf{K}_1(\boldsymbol{\eta}_i, \Delta\boldsymbol{\eta}_i) + \mathbf{K}_2(\boldsymbol{\eta}_i, \Delta\boldsymbol{\eta}_i) + \frac{1}{4}\mathbf{K}_2(\Delta\boldsymbol{\eta}_i, \Delta\boldsymbol{\eta}_i) \right] \Delta\boldsymbol{\eta}_i = \Delta\lambda_i \mathbf{F} \quad (54)$$

where \mathbf{F} is the reference load vector. The iterative form of Eq. (54) for the r -th iteration of the i -th step follows:

$$\mathbf{K}_i^r \Delta\Delta\boldsymbol{\eta}_i^r = \Delta\Delta\lambda_i^r \mathbf{F} - \Delta\mathbf{R}_i^r \quad (55)$$

in which

$$\begin{aligned} \Delta\Delta\boldsymbol{\eta}_i^r &= \Delta\boldsymbol{\eta}_i^{r+1} - \Delta\boldsymbol{\eta}_i^r \\ \Delta\Delta\lambda_i^r &= \Delta\lambda_i^{r+1} - \Delta\lambda_i^r \end{aligned} \quad (56)$$

and

$$\begin{aligned} \mathbf{K}_i^r &= \mathbf{K}_{0i} + \mathbf{K}_1(\boldsymbol{\eta}_i, \Delta\boldsymbol{\eta}_i^r) + 2\mathbf{K}_2(\boldsymbol{\eta}_i, \Delta\boldsymbol{\eta}_i^r) + \mathbf{K}_2(\Delta\boldsymbol{\eta}_i^r, \Delta\boldsymbol{\eta}_i^r) \\ \Delta\mathbf{R}_i^r &= \left[\mathbf{K}_{0i} + \frac{1}{2}\mathbf{K}_1(\boldsymbol{\eta}_i, \Delta\boldsymbol{\eta}_i^r) + \mathbf{K}_2(\boldsymbol{\eta}_i, \Delta\boldsymbol{\eta}_i^r) + \frac{1}{4}\mathbf{K}_2(\Delta\boldsymbol{\eta}_i^r, \Delta\boldsymbol{\eta}_i^r) \right] \Delta\boldsymbol{\eta}_i^r - \Delta\lambda_i^r \mathbf{F} \\ \mathbf{K}_{0i} &= \mathbf{K}_0 + \mathbf{K}_1(\mathbf{0}, \boldsymbol{\eta}_i) + \mathbf{K}_2(\boldsymbol{\eta}_i, \boldsymbol{\eta}_i). \end{aligned} \quad (57)$$

At this point, appropriate shape functions for the trial and test functions are assumed in order to discretize equation Eq. (55). In the quasi-conforming shell element the shape functions of Tang [5] are used for the discretization of the linear strain $\epsilon_o^{(1)}$, the total curvature change κ' , the rotations ϕ of the mid-surface and displacements. The modified Newton-Raphson method and arc length approach (Riks [4]; Zhang and Atluri [6]) are used to solve Eq. (55). At bifurcation points on paths, the asymptotic post-buckling solutions are taken as the initial values of iteration, so that any assumed imperfections are rendered unnecessary.

5 NONLINEAR SOLUTION SCHEMES

Automated post-buckling solution involves: detection of possible instability in solution and elimination of possible path-retracing; classification of the detected instabilities; and computation of the post-through buckling solution(s). BUCKDEL detects solution instabilities by monitoring the rank of the tangent stiffness matrix. Whenever the determinant of the tangent stiffness matrix changes its sign the solution senses possible instabilities in that range of load and changes the sign of the next load increment to avoid path-retracing. Through a cycle of iterations, location of instabilities are identified as the load levels for which the tangent stiffness becomes singular. The identified instability points are then

classified as limit points or bifurcation points using some simple and cost-effective rules (Huang and Atluri [3]). If the instability point is a limit point, the *arc-length continuation* is enough to obtain post-buckling solution path. However, if the instability point happens to be a bifurcation point, the strategies described in detail in [3] are used to trace the appropriate post-buckling solution branch. The nonlinear fundamental state between the two solution points $n - 1$ and n in the neighborhood of the bifurcation point is *linearized* to obtain the *asymptotic* solution for obtaining an approximate critical buckling load factor. A linear combination of the *normalized* eigen-vector associated with the critical buckling load factor and its orthogonal counterpart is used to determine the initial post-buckling paths.

6 POINTWISE ENERGY RELEASE RATE CALCULATION

In the case of delamination, the growth is assumed to be along the interlaminar zone parallel to the midsurface of the shell (i.e. the crack cannot shear into the neighboring laminae). Since the displacement field is made explicitly continuous at the delamination front, the delaminate shell cannot slide or rotate relative to the base shell. Hence, the J-integral representing only *self-similar* crack growth is meaningful in the present case.

The pointwise energy release rate for 3-dimensional crack growth (self-similar) - $\mathcal{G}(\Gamma)$ - is defined as,

$$\mathcal{G}(\Gamma)\Delta\Gamma = \lim_{e \rightarrow 0} \int_{A_e} \left[W\bar{n}_1 - \bar{\sigma}_{\alpha\beta}\bar{n}_\beta \frac{\partial \bar{U}_\alpha}{\partial \bar{x}_1} \right] dA + \int_{A_1} \bar{\sigma}_{\alpha 2} \frac{\partial \bar{U}_\alpha}{\partial \bar{x}_1} dA - \int_{A_2} \bar{\sigma}_{\alpha 2} \frac{\partial \bar{U}_\alpha}{\partial \bar{x}_1} dA \quad (58)$$

where, $\alpha, \beta = 1, 2, 3$; A_e is the area of the tube of radius e enclosing the crack front; A_1 and A_2 are the areas covering the ends of the tube; and \bar{n} , $\bar{\sigma}$, \bar{U} and \bar{n} are defined in the crack tip coordinate system \bar{x} (Figure 4).

Consider a rectangular tube enclosing the delamination front and passing through the nearest stress recovery points ($S^{(i)}$) of the adjoining elements (Figure 4). Note that, the integrals over the areas A_1 and A_2 nearly cancel each other in a constant strain/stress element model, since the quantities like $\bar{\sigma}$ and $\partial \bar{U}_\alpha / \partial \bar{x}_1$ do not vary in the neighborhood of a point in an element domain. Then, equation (58) for the self-similar delamination growth becomes,

$$\mathcal{G}(\Gamma)\Delta\Gamma = \int_{\Delta\Gamma} \sum_{j=1}^9 \int_{\Lambda_j} \left(W\bar{n}_1 - \bar{\sigma}_{\alpha\beta}\bar{n}_\beta \frac{\partial \bar{U}_\alpha}{\partial \bar{x}_1} \right) d\Lambda d\Gamma \quad (59)$$

where Λ_j ($j = 1 - 9$) are the segments forming the surface area A_e of the rectangular tube (Figure 4). Since the Reissner-Mindlin assumptions ($\bar{\sigma}_{13}, \bar{\sigma}_{23}$ are constant over shell thickness; and $\bar{\sigma}_{33} = 0$) are used for the element formulations as well as to achieve displacement continuity at the delamination edge; and since $\bar{n} = \{0 \ 0 \ \pm 1\}$ on the segments Λ_j , $j = 4 - 9$ (see Figure 4), the integral in equation (59) vanishes over the segments Λ_j , $j = 4 - 9$. Now, since $\bar{n} = \{+1 \ 0 \ 0\}$ on the segment Λ_1 and

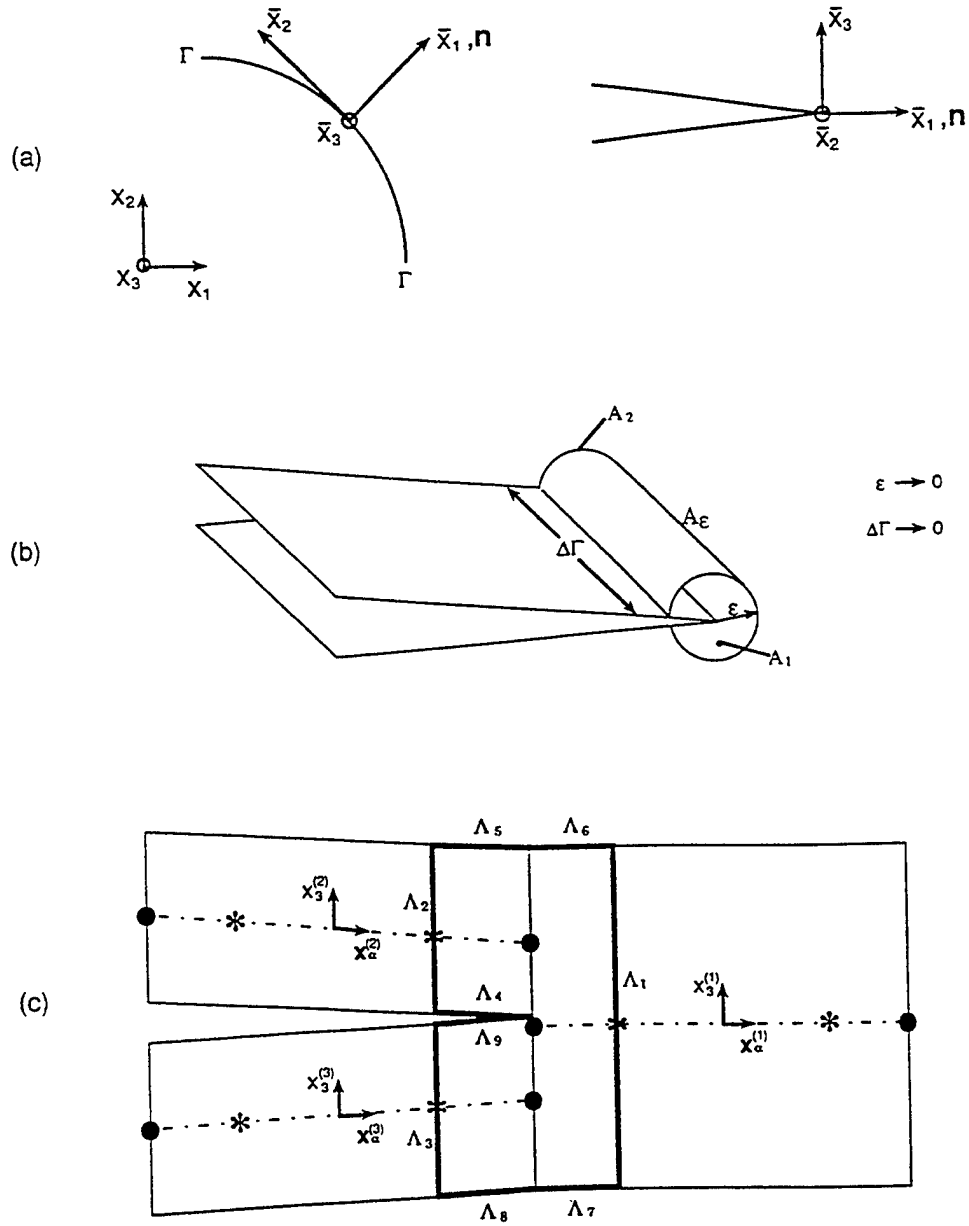


Figure 4: Energy release rate computation in multi-domain model

$\bar{n} = \{-1 \ 0 \ 0\}$ on the segments Λ_2 and Λ_3 ; equation (59) becomes,

$$\mathcal{G}(\Gamma)\Delta\Gamma = \int_{\Delta\Gamma} \left[\int_{\Lambda_1} - \int_{\Lambda_2} - \int_{\Lambda_3} \left(W - \bar{\sigma}_{\alpha 1} \frac{\partial \bar{U}_{\alpha}}{\partial \bar{x}_1} \right) dx_3 \right] d\Gamma \quad (60)$$

Now, carrying out the integration through the thickness for each shell, we get,

$$\mathcal{G}(\Gamma)\Delta\Gamma = \int_{\Delta\Gamma} \mathcal{F}_g \left[\hat{W} - \left(\bar{N}_{1\alpha} \bar{u}_{\alpha,1} + \bar{M}_{1\alpha} \bar{\theta}_{\alpha,1} + \bar{Q}_{13} \bar{u}_{3,1} \right) \right] d\Gamma \quad (61)$$

Therefore, as $\Delta\Gamma \rightarrow 0$, the pointwise energy release rate at any point on the delamination front \mathcal{G}_g , computed from the Gauss-point variables, in a finite element model using constant strain elements, is given by,

$$\mathcal{G}_g(\Gamma) = \mathcal{F}_g \left[\hat{W} - \left(\bar{N}_{1\alpha} \bar{u}_{\alpha,1} + \bar{M}_{1\alpha} \bar{\theta}_{\alpha,1} + \bar{Q}_{13} \bar{u}_{3,1} \right) \right] \quad (62)$$

where, $\mathcal{F}_g(*) = (*)_{g(1)} - (*)_{g(2)} - (*)_{g(3)}$ and $(*)_{g(i)}$ corresponds to the quantities $(*)$ evaluated at specified points on the annular surface. For example, in a finite element analysis, these specified points would be preferably the optimal stress recovery points - normally the Gauss points corresponding to reduced integration - in the adjoining element of the i^{th} shell nearest to the delamination front Γ .

Note that when energy release rate calculations are performed with BUCKDEL, the finite element mesh adjoining the delamination edge should be symmetric about the delamination edge such that (a) the stress recovery points for all the elements are at the same radial distance from the delamination edge; and (b) each set of elements from the three shells should have stress recovery points located on a single plane normal to the delamination front.

References

- [1] S. N. Atluri, B.Z. Huang, and V.B. Shenoy. A quasi-conforming triangular laminated composite shell element based on a refined first-order theory. Technical Report FAA Center of Excellence Report, Georgia Institute of Technology, 1993.
- [2] S.N. Atluri, P. Tong, and H. Murakawa. Recent studies on hybrid and mixed finite element methods in mechanics. In *Hybrid and Mixed Finite Element Methods*, pages 51-71. Wiley, 1983.
- [3] B.Z. Huang and S.N. Atluri. A simple method to follow post-buckling paths in finite element analysis. *Computers and Structures*, 57:477-489, 1995.
- [4] E. Riks. The application of newton's method to the problem of elastic stability. *Journal of Applied Mechanics*, 39:1060-1066, 1972.
- [5] L.M. Tang. Quasi-conforming elements for finite element analysis. *Journal of the Dalian Institute of Technology*, 19:135-147, 1980.
- [6] J. D. Zhang and S. N. Atluri. Non-linear quasi-static and transient response analysis of shallow shells: Formulations and interior/boundary element algorithms. In Q. Du, editor, *Boundary Elements*, pages 87-109. Pergamon Press, 1986.